UNIVERSITY OF CALIFORNIA, SAN DIEGO

G protein-coupled receptor expression and function in cancer and the cancer-associated microenvironment: A study of Chronic Lymphocytic Leukemia and Pancreatic Adenocarcinoma

A Thesis submitted in partial satisfaction of the requirements for the degree of Master of Science

in

Biology

by

Thalia McCann

Committee in charge:

Professor Paul Insel, Chair
Professor Stephen Hedrick, Co-Chair
Professor Shannon Lauberth

2015

The Thesis of Thalia McCann is approved, and it is acceptable in quality and form for publication on microfilm and electronically:

_____

_____

Co-Chair

_____

Chair

University of California, San Diego

2015

DEDICATION

I would like to dedicate the work of this thesis to my beloved Grandpa Jack, who passed away too soon from cancer of the pancreas; may our research help to prevent others from the same fate.

EPIGRAPH

“Science makes people reach selflessly for truth and objectivity; it teaches people to accept reality, with wonder and admiration, not to mention the deep awe and joy that the natural order of things brings to the true scientist.”

-Lise Meitner

TABLE OF CONTENTS

LIST OF FIGURES

LIST OF TABLES

LIST OF SUPPLEMENTAL FIGURES

LIST OF SUPPLEMENTAL TABLES

ACKNOWLEDGEMENTS

I would like to express my gratitude to Dr. Paul Insel for his support as the chair of my committee. Throughout the past three years, I have been extremely fortunate to have Paul as my advisor. He gave me the invaluable opportunity to participate in novel research, but he has also shown unparalleled enthusiasm and an unwavering commitment to education and science research.

I would also like to acknowledge my mentors, Ross Corriden, Shu Zhou, and Andrea Wilderman, for their guidance, encouragement, and support throughout the duration of my time in the lab. Andrea's devotion to teaching gave me with motivation and inspiration to pursue science research. Shu's attention to detail and drive for perfection challenged me to become a better scientist and to produce high quality results. Ross's guidance and mentorship provided a constant source of encouragement and helped me to craft a superior thesis.

I would like to thank Nakon Aroonsakool and the rest of the Insel Lab for all the help, patience, and education they have given me.

I would like to thank my parents for their love, devotion, and incredible support throughout my years in graduate school. I would especially like to thank Giovanni Hanna for the encouragement to both pursue and complete this degree, and for all of his help along the way. I would also like to thank my friends, especially Ronnie Steinitz for her generous help with formatting, and the

wonderful support that she and Lindsay Bailey have given me over the past three years.

Finally, I would like to acknowledge and thank Dr. Stephen Hedrick and Dr. Shannon Lauberth for taking the time to serve on my thesis committee.

ABSTRACT OF THE THESIS

G protein-coupled receptor expression and function in cancer and the cancer-associated microenvironment:
A study of Chronic Lymphocytic Leukemia and Pancreatic Adenocarcinoma

by

Thalia McCann

Master of Science in Biology

University of California, San Diego, 2015

Professor Paul A. Insel, M.D., Chair

Professor Stephen Hedrick Co-Chair

G protein-coupled receptors (GPCRs) are the largest superfamily of membrane receptors and are targeted by more than 30% of FDA-approved drugs. Although there has been limited study of GPCRs in cancer, they may be strategic targets in treating both tumor cells and the supportive microenvironment that is implicated in malignancies such as chronic lymphocytic leukemia (CLL)

and pancreatic ductal adenocarcinoma (PDAC). In this thesis research, TaqMan® GPCR arrays were used as an unbiased approach to characterize the GPCR profile of CLL cells and NKtert bone marrow cells, as well as PDAC cells and pancreatic- cancer associated fibroblasts (CAFs). The results revealed that targeting two highly expressed G_s-linked GPCRs, VIPR1 and MC2R, in combination with the dual PDE inhibitor IR284, increased CLL cell death, presumably by increasing cellular cAMP levels. I characterized the GPCR profile of bone marrow NKtert cells and found that cAMP-mediated effects reduce NKtert cell viability and proliferation by modulation of protein kinase A (PKA) and the Exchange Protein activated by cAMP -1 (Epac-1), respectively. I determined that PDAC cells express 73 GPCRs whose expression was shared on three patient tumors, and 55 GPCRs shared between two patient-derived cell lines and two PDAC cell lines. Of these GPCRs, the Class C orphan GPRC5A was found to be the most highly expressed and up-regulated in PDAC cells relative to a normal pancreatic ductal epithelial cell line (HPDE6) and in CAFs compared to pre-fibroblast precursor cells (pancreatic stellate cells, PSC). Transfection of HPDE6 cells with GPRC5A enhanced DNA synthesis in the cells, indicating that GPRC5A may contribute to the malignant phenotype of PDAC and may be a novel therapeutic target for pancreatic cancer. Thus, I was able to characterize the expression of GPCRs in two types of cancer, in both the cancer cells themselves and in cells of their associated microenvironment. The findings provide new insights regarding GPCR expression in cancer and suggest new ways in which cancer cells interact with their surrounding microenvironment.

1. Introduction

1.1 G protein-coupled receptors

G-protein-coupled receptors (GPCRs), also known as heptahelical or 7-transmembrane receptors, are a superfamily of signaling receptors comprising approximately 800 genes in the human genome[1]. GPCRs are expressed throughout the body, modulate diverse cellular processes, and respond to a variety of endogenous signals such as neurotransmitters and hormones[1–3]. There are 430 GPCRs responsible for sensing exogenous signals such as light, odorants, and tastes[1–3]. Of the remaining 369 GPCRs, many play important roles in pathophysiology or as therapeutic targets of human diseases; in fact, >30% of current FDA- approved pharmacological agents target GPCRs[4]. Tissue specificity and ligand selectivity, along with the accessibility of the receptors from the extracellular milieu, make GPCRs particularly appealing targets. However, physiological agonists remain unknown for more than 120 GPCRs (termed “orphan” GPCRs) and thus have been largely ignored in drug development; such “untapped” receptors may be important novel therapeutic targets[1,3,5].

Membrane-localized GPCRs, when bound by agonist ligands, change conformation and activate their associated heterotrimeric guanine nucleotide binding proteins (G-proteins)[1]. Upon activation, G-protein βγ and α subunits separate from each other, and both the βγ dimer and α subunit are able to regulate downstream effector pathways. For example, membrane-bound βγ

activates ion channels[6]. The signaling pathway of the α subunit determines the class of the G-protein ($G\alpha_s$, $G\alpha_i$, $G\alpha_{q/11}$, $G\alpha_{12/13}$). $G\alpha_s$ stimulates adenylyl cyclase, which synthesizes cAMP, while $G\alpha_i$ inhibits adenylyl cyclase activity, resulting in decreased cellular cAMP concentrations. $G\alpha_{q/11}$ signaling activates phospholipase Cβ to cleave phosphatidylinositol 4,5,-bisphosphate into inositol (1,4,5)-trisphosphate and diacylglycerol, which, respectively, stimulate Ca2+ release from the endoplasmic reticulum and activate protein kinase C. $G_{12/13}$ activates RhoA, a GTPase that plays important roles in actin-myosin contractility and cell migration, as well as cell-cycle control[4,7,8,9,10]. GPCR signaling can be modulated by the activity of G-protein receptor kinases (GRKs), β-arrestins, allosteric modulators and by homo-/hetero-dimerization of GPCRs[4]. In addition, GPCRs can transactivate receptor tyrosine kinases such as the epidermal growth factor receptor (EGFR)[4,11,12].

1.1 GPCRs in cancer

GPCRs have been studied in the context of many different diseases but their role in cancer has been largely underappreciated. However, a growing body of literature has begun to establish such a role. GPCRs are able to modulate cell cycle progression, apoptosis, differentiation, tissue vascularization, cellular motility and migration, processes that play critical roles in the pathophysiology of cancer[4]. For example, thrombin, lysophosphatidic acid, and neuropeptides can propagate mitogenic signals through GPCRs, thus influencing cancers of the

breast, ovaries, lung, and prostate[8]. GPCRs can be activated by oncogenic viruses that contribute to Kaposi sarcoma, nasopharyngeal sarcoma, and various lymphomas[7,8]. Autocrine effects and paracrine GPCR signaling between tumor and stromal cells have been identified in multiple cancers. For example, prostaglandin signaling associated with inflammation results in activation of EP2 and EP4 GPCRs and has been linked to accelerated growth, angiogenesis and metastasis in multiple tumor types[7,8]. The actions of chemokine GPCRs have been shown to regulate cancer metastasis and migration; most notably, CXCR4 signaling through stromal cell-derived factor 1 (SDF-1) influences multiple cancers, including chronic lymphocytic leukemia (CLL)[4,8,13]. Furthermore, treatment of pancreatic cancer cells with a broad-spectrum GPCR antagonist greatly blunted proliferation and angiogenesis[14]. For these reasons, an underlying hypothesis of this thesis is that GPCRs may be important regulators of the function of cancer cells and cells in the tumor microenvironment (Figure 1.1) and thereby, may be therapeutic targets to disrupt interactions between tumors and their supporting microenvironment.

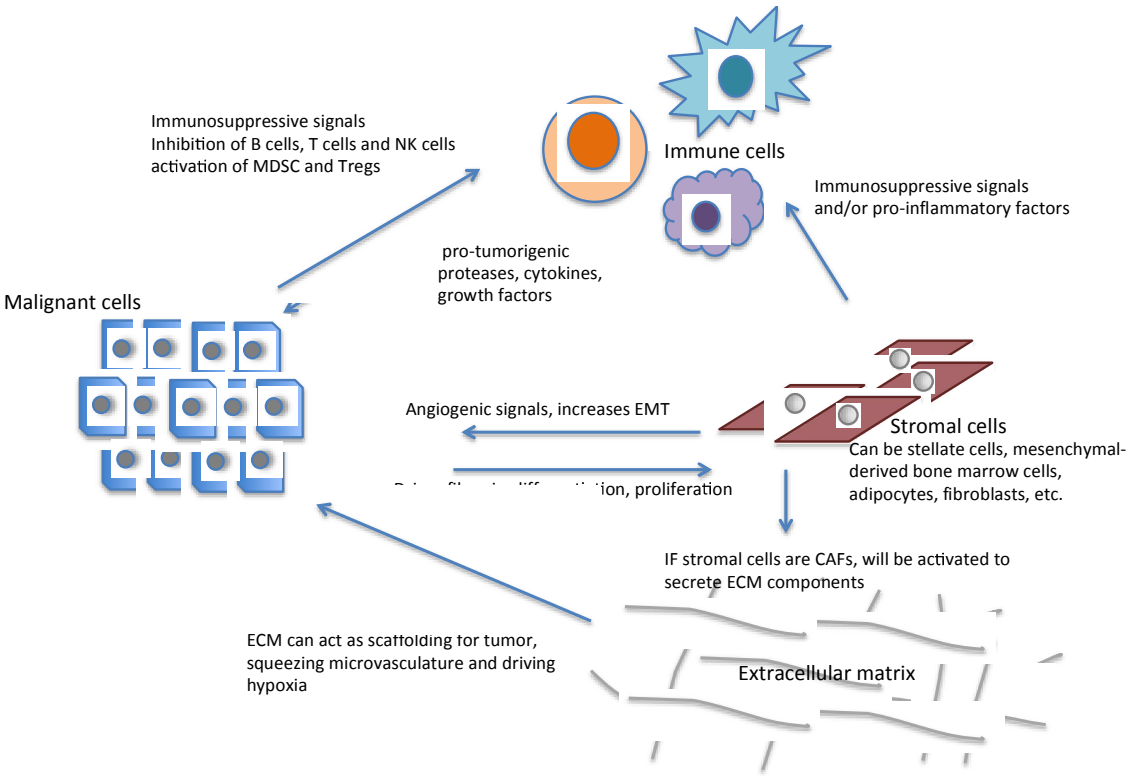

Figure 1.1 Overview of cancer-microenvironment interactions between stromal cells, immune cells and cancer cells that enhance the malignant phenotype. Immune cells include tumor-associated macrophages (TAMs), B and T cells (tumor infiltrating lymphocytes, TILs), dendritic cells as well as myeloid-derived suppressor cells (MDSC) which act with certain regulatory T cells (Tregs) to be immunosuppressive. Stromal cells include multiple cell types and generally depend on the tumor's tissue of origin.

2. Materials and Methods:

2.1 Cell culture:

B cells from patients with CLL or normal B cells (provided by Dr. T. Kipps, Moores Cancer Center) were cultured in RPMI 1640 (Gibco Life technologies, Grand Island, NY) with 10% Heat-inactivated Fetal Bovine Serum (FBS) (Omega Scientific, Tarzana, CA). NK.tert cells are human bone marrow cells immortalized with human telomerase reverse transcriptase (hTERT) and were cultured in DMEM with L-glutamine and 10% FBS.

Patient-derived PDAC whole tumors were surgically removed and tissue samples were frozen in liquid nitrogen or explanted, allowing for the isolation of CAFs by outgrowth on matrigel, from which RNA was prepared and provided by Dr. A Lowy (Moores Cancer Center). Patient-derived cell lines 79E and 34E were derived from patient tumors that were xenografted in a NSG mouse and then explanted and isolated for culture (provided by Dr. A. Lowy,). 79E and 34E were grown in DMEM (Gibco Life technologies) with 10% FBS, 4.5 g/L glucose, 2 mM L-glutamine, 1 mM Sodium Pyruvate, 1x Non-essential amino acids (NEAA) (Gibco Life technologies), 2x Penicillin/ Streptomycin (P/S) (Gibco Life technologies).

Aspc-1 (American Type Culture Collection [ATCC], Manassas, VA) were grown in RPMI 1640 10% FBS (Omega Scientific). MiaPaCa-2 (ATCC) were grown in high glucose DMEM + L-glutamine with 10% FBS. An immortalized normal pancreatic ductal epithelial cell line in which the E6E7 genes from human papilloma virus (HPV) were transfected (HPDE6) (provided by Dr. A. Lowy) were

grown in Keratinocyte Serum Free media (KSFM) with Bovine Pituitary Extract (BPE) and Epidermal Growth Factor (EGF) supplements (Gibco Life technologies) [15]. All cells cultured in 37°C air with 5% CO_2.

2.2 Small-Molecule Agonists/Antagonists and Chemical Reagents:

Staurosporine (Sigma St. Louis, MO) is a ATP-competitive kinase inhibitor that induces apoptosis.[16] IR284 (4-(3-chloro-4-methoxyphynyl)-2-(1-morpholine-4-carbonyl) piperadin-4-yl)-4a, 5,88a-tetrahydrophthalazin-1(2H)-one, CSD Cancer Center Medicinal Chemistry Core, UCSD) is a PDE 4/7 dual inhibitor known to raise cAMP levels in CLL cells.[17,18] Vasointestinal Peptide (VIP) (Tocris Bioscience, Minneapolis, MT) is the agonist of Vasointestinal Peptide Receptor 1 (VIPR1).[19] Adrenocorticotropic hormone (ACTH) (Genway, San Diego, CA) is the agonist of Melanocortin receptor 2 (MC2R)[20]. β-Mercaptoethanol (BME) (Sigma) is a reducing agent that inhibits the oxidation of free sulfhydryl residues[21]. TCEP (*tris*(2-carboxyethyl)phosphine) (Sigma) reduces disulfides.[22] CPT (8-(4-Chlorophenylthio)adenosine-5'-O-monophosphate) is a cAMP analog[23]. 8ME (8-(4-Chlorophenylthio)-2'-O-methyladenosine 3',5'-cyclic Monophosphate) is a cAMP analog that is a selective EPAC activator[24]. N6 (N^6-Phenyladenosine-3',5'-cyclic monophosphate) (all cAMP analogs were obtained from Axxora, Farmindale, NY) is a cAMP analog that is a selective activator of PKA[25]. Dimethyl sulfoxide (DMSO) (Alfa Aesar, Ward Hill, MA) is a polar aprotic solvent used to solvate several drugs listed above and serves as a vehicle control.

2.3 Flow cytometry/ FACS analysis of CLL B cell apoptosis:

Drug- induced apoptosis:

1 x10^5 B cells from individual CLL patients (with aggressive or Indolent CLL, as indicated) were seeded per well in a 24 well plate in RPMI 1640 + 10% FBS (Omega Scientific) for 48 hours. Cells were treated with 100 nM IR284 +/- 1 μM VIP or 100 nM IR284 +/- 1 nM ACTH.

Viability due to stromal interaction or reduction:

1 x10^5 B cells from patients with aggressive CLL were resuspended in RPMI 1640 + 10% FBS and co-cultured with 1 x 10^5 NKtert stromal cells or treated with NKtert conditioned media, 20 μM βME, or 20 μM TCEP for 48 hours.

Cells were pelleted, washed with cold phosphate buffered saline (PBS) with 1% FBS, resuspended in 100 μL Hank's Balanced Salt Solution (HBSS) (Invitrogen, Carlsbad CA) and stained with Annexin V/ fluorescein isothiocyanate (FITC) (Becton Dickinson Biosciences), propidium iodide and CD19-PE (phycoerythrin) (Caltag Laboratories, Burlingame, CA) in HBSS. Each sample was analyzed by flow cytometry (FACScan, Becton Dickinson Biosciences). Single stained controls were used to set gates for analysis of viable (lower left quadrant) versus apoptotic populations with high Annexin V staining (upper and lower right quadrants). Relative mortality was calculated as percent gated with

high Annexin V staining, and drug-induced mortality was calculated as a percentage normalized to basal apoptosis of the untreated control.

2.4 Statistical Analysis:

Drug-induced apoptosis was assessed using a 1-way ANOVA with Fischer's Least Standard Deviation test. Viability due to stromal interaction or reduction was assessed using a 1-way ANOVA with Tukey's post-hoc analysis. Statistical significance was considered for p values < 0.05.

2.5 Viability by MTT assay:

NKtert cells were treated with H_2O, 2 μM Staurosporine, 10 or 100 μM CPT, 10 or 50 μM 8ME, or 10 or 50 μM N6 for 24 hours. MTT (3-(4,5-dimethylthiazol-2-yl)-2,5-diphenyltetrazolium bromide) (Life technologies) (0.5 mg/mL in PBS) was added to 1 $x10^5$ cells per well in a 12 well plate for 4 hours. The resulting MTT formazan was solubilized in 1 mL acidic isopropanol and 200 μL of supernatant was moved to a clear bottom 96-well plate for absorbance measurement at O.D. 570 and 630 in a DTX-800 Plate Reader (Beckman Coulter), where signal was computed by subtracting background ($O.D._{570}$ – $O.D._{630}$) for each sample.

2.6 Viability by CellTiter Glo Assay:

2.5 x 10^5 transfected HPDE6 cells were seeded in each well of a 96-well plate in KSM with EGF and PBE. Viability was assessed after 48 hours using the

CellTiter-Glo assay (Promega, Madison, WI) according to the manufacturer's instructions.

2.7 Transfection:

HPDE6 cells were grown in 10-cm dishes until confluent and then treated with 2.8 μg plasmid (GeneCopoeia, Rockville, MD) and 11.2 μL FuGENE transfection reagent (Promega) in a total volume of 200 μL OptiMEM Serum-Free media (Gibco Life technologies).

2.8 RNA isolation and cDNA Synthesis:

Patient tumor tissue (10 mg; provided by Dr. A. Lowy) loaded with 350 μL RLT buffer into a QiaShredder column (Qiagen, Venlo Limburg, Netherlands) and centrifuged for 2 minutes at >8,000 x g. RNA was isolated using a Qiagen RNeasy MiniKit, and cDNA was synthesized using Superscript III First Strand Synthesis Kit (Invitrogen, Carlsbad, CA) as per the manufacturer's instructions.

2.9 TaqMan® Human GPCR Arrays:

GPCR expression profiles were determined using TaqMan GPCR arrays (Applied Biosystems Life technologies) in collaboration with the CFAR Genomic Core (UCSD). For each array, 1 ng/μL of cDNA in Taqman® Universal PCR Master Mix was loaded into a 384-well microfluidic card. Exponential curves for each detector were investigated using RQ manager software, and abnormal or flagged amplifications were marked as "undetected" and omitted from further

analysis. GPCRs that showed no amplification by C(t)= 40 were considered not detected. Expression was normalized to the average of four 18S rRNA cyclic threshold (C(t)) values as $\Delta C(t) = C(t)_x - C(t)_{18S}$ for each GPCR detector (x).

2.10 Quantitative PCR (qPCR):

Primers were designed using the NCBI Entrez search engine (http://www.ncbi.nlm.nih.gov/sites/entrez) and purchased from ValueGene. PDE isoform primers were identical to those used by Zhang et al [17]. Template cDNA (8 ng), 200 nM forward and reverse primers, and qPCR Mastermix Plus for Sybr Green I (Eurogentec, San Diego, CA) were combined and loaded into a white 96-well qPCR plate. Fluorescence was measured using an Opticon 2 RT-PCR machine (MJ Research, Waltham, MA). Samples were compared using cycle threshold values (Ct) normalized to either 28S or 18S rRNA

Table 2.1 real-time qPCR thermocycler protocol

Step	Temperature (°C)	Time
1	50	2 min
2	95	10 min
3	95	15 sec
4	60	30 sec
5	72	1 min
6	Plate read.	
Go to Step 3 34 more times.		
7	Construct melting curves for samples by heating the plate from 60°C to 95°C. Read plate every 0.2°C, holding the temperature for 1 sec.	

Table 2.2 Primers used in qPCR assays

Gene	Forward primer (5’ to 3’)	Reverse primer (5’ to 3’)	T_m °C
18S	aaacggctaccacatccaag	cctccaatggatcctcgtta	60
28S	gcctagcagccgacttagaa	aaatcacatcgcgtcaacac	60
PKA RIa	gggaagcacactgagaaagc	acagcagctgacccctctaa	60
PKA RIIa	gtcaaagatggggagcatgt	agcaccaggagaggtagcag	60
EPAC-1	actttatccccaacttggat	tcctccagaaactctcagac	60
GPRC5A	gccttcatcatcggactggac	agcgataacatcctggactagg	60

2.11 [^{3}H] Thymidine Incorporation Assay:

Twenty-four hours following transfection, 1 x10^5 HPDE6 cells or NKtert stromal cells were seeded in a six-well plate; the following day cells were serum-starved. After an additional 24 hours, KSFM + BPE and EGF were added to HPDE6 cells, or RPMI 1640 + 10% FBS conditioned by CLL cells that were treated for apoptosis analysis as described (2.3) was added to NKtert stromal cells. [^{3}H]Thymidine (1 μCi/mL final) was added. After 48 hour incubation at 37ºC with 5% CO_2, cold 7.5% trichloroacetic acid (TCA) (Alfa Aesar, Ward Hill, MA) was added. The resulting precipitate was dissolved in 1 mL 0.5 M NaOH and combined with 3 mL of scintillation fluid. Counts-per-minute were measured for each sample for 1 minute using a Beckman Coulter LS 1801 scintillation counter.

2.12 GEO Profile for GPRC5A expression profile in Pancreatic Cancer:

Gene Expression Omnibus (GEO) (http://www.ncbi.nlm.nih.gov/geoprofiles/).

2.13 TCGA profile for GPRC5A alterations and expression:

cBioPortal for Cancer Genomics (http://www.cbioportal.org/)

2.14 Prediction of GPCR linkage:

GPRC5A linkage was predicted using PredCouple2 (http://athina.biol.uoa.gr/bioinformatics/PRED-COUPLE2/).

2.15 Computational Modeling of GPRC5A:

I-TASSER was used to generate a 3D model of GPRC5A (Zhang Lab, University of Michigan).

3. GPCRs in Chronic Lymphocytic Leukemia and bone marrow stromal cells

3.1 Introduction

3.1.1 B Cell Chronic Lymphocytic Leukemia

Chronic Lymphocytic Leukemia (CLL) is the most common adult leukemia in the Western world, with an estimated 14,620 new cases and 4,650 deaths expected in the U.S. in 2015[26]. CLL is characterized by the accumulation of malignant B cells in the peripheral circulation and lymphoid tissues[27,28]. This accumulation occurs because malignant CD19+, CD20+, CD5+, CD23+, and CD27+ B cells are arrested in G_0/G_1 phase and have decreased programmed cell death, or apoptosis[29,30]. CLL cells express high amounts of anti-apoptotic proteins, specifically those of the Bcl-2 family, which may contribute to this anti-apoptotic feature[30]. The majority of circulating CLL cells are growth-arrested but a small proportion of CLL cells divide in proliferating centers within lymph nodes or the bone marrow, suggesting that B-CLL is a dynamic disease, in which the microenvironment plays an important role[28,29]. There is as yet no cure for CLL.

CLL is a clinically heterogeneous disease that is classified on the basis of two independent studies (from 1975 and 1977) that defined three patient groups with different prognostic outcomes: 1) early asymptomatic CLL (Rai stage 0 or Binet class A) with survival of more than 10 years; 2) intermediate risk CLL (Rai I-II or Binet B) with approximately 7 year survival; 3) high risk CLL (Rai III-IV or Binet C) with less than 4 year survival [31,32]. Molecular characterization of B-CLL

has divided patients into two groups based on IgV_H mutation status and surface markers: *aggressive* CLL patients have non-mutated IgV_H (or <2% variation from germline V genes); and high expression of the tyrosine kinase zeta-associated protein of 70 kDa (ZAP70) and CD38, which correlate with poorer prognosis, such that these patients succumb to the disease at three-times the rate of patients with *indolent* CLL[29]. However, no single prognostic marker has been able to directly track disease progression across the heterogeneous population of CLL patients and the mechanisms that drive the malignant phenotype in CLL have not been fully defined.

3.1.2 Targeting cAMP in CLL

3',5' cyclic adenosine monophosphate (cAMP) is a second messenger that is produced by adenylyl cyclase upon activation by G protein-coupled receptor (GPCR) signaling cascades. cAMP regulates numerous cellular functions primarily through its ability to modulate the activity of two principal effectors: protein kinase A (PKA) and the exchange protein directly activated by cAMP (Epac)[33]. cAMP levels are regulated by the activity of 3', 5'-cyclic phoshodiesterases (PDEs) that hydrolyze cAMP to 5' adenosine monophosphate (AMP) and therefore limit the extent and duration of cAMP-mediated signaling[34]. Levels of PKA and cAMP are lower, while Epac-1 and PDE7B expression are more abundant in CLL cells than in normal peripheral blood mononuclear cells (PBMCs) [18,35]. This suggests that changes in the expression of cAMP-related

signaling components may contribute to the pathophysiology of CLL B-cells[35]. Previous work has shown that cAMP signaling
via PKA increases the expression of pro-apoptotic proteins, reduces the expression of pro-survival proteins, and results in mitochondria-dependent apoptosis in CLL[36,37]. PDE4, PDE7 or dual PDE4/7 inhibitors, such as IR284, can increase cAMP and induce apoptosis in CLL cells through PKA-mediated actions[18,17,38]. Conversely, the actions of Epac-1 are anti-apoptotic in CLL cells[38]. Based on the ability of PKA to promote apoptosis, targeting GPCRs to increase intracellular cAMP in combination with PDE- targeted inhibitors may be a way to treat CLL.

3.1.3 Mesenchymal bone marrow stromal cells in CLL

Mesenchymal-derived bone marrow stromal cells (BMSCs) are a major contributor to the microenvironment that interacts with CLL-B cells, along with T-cells and monocyte-derived nurse-like cells. BMSCs play an important role in supporting hematopoiesis[39]. In CLL, the bone marrow provides a protective niche; CLL cells are attracted to the bone marrow and lymphoid tissues by chemokines secreted by BMSCs, where clonal populations are replenished in proliferating centers and signals from BMSCs assist the CLL cells in evading drug-induced apoptosis[40,41,42]. CLL cell protection by its milieu accomplice allows for persistent minimal residual disease after treatment in the marrow niche and ultimately facilitates the clonal expansion of CLL cells that are resistant to

therapy and relapse[43,44]. The extent of marrow infiltration correlates with the prognosis of CLL patients[43,45].

3.1.4 Hypothesis and Goals

Hypothesis One

Previous work in the Insel laboratory identified two highly expressed G_s-linked GPCRs in CLL, VIPR1 and ACTH, which stimulate cAMP-induced apoptosis in CLL cells. I hypothesized that treatment of cells from additional indolent and aggressive CLL patients with ligands for these GPCRs would promote apoptosis of CLL cells.

Hypothesis Two

Characterization of the bone marrow stromal cells will further understanding of their response to cAMP-stimulating treatments (e.g., PDE inhibitors or GPCR agonists). Studies of the stromal cells may also facilitate the identification of targets such as GPCRs or PDEs that would identify novel therapeutic strategies for CLL that could disrupt the bone marrow-CLL cell survival axis (Figure 1.1).

3.2 Results part I: Targeting GPCRs to increase apoptosis in CLL cells

Prior work by Insel laboratory member Trishna Katakia included TaqMan® GPCR array analysis of samples pooled from indolent and aggressive CLL patients. The results showed that VIPR1 and MC2R are two G_s-linked GPCRs with the largest increase in expression in CLL cells compared to normal B cells and by comparison of indolent and aggressive CLL cells. VIPR1 had increased expression in aggressive CLL cells relative to both normal B cells ($\Delta\Delta$Ct = 4.5) and indolent CLL cells ($\Delta\Delta$Ct = 9.5). MC2R showed higher expression in both indolent and aggressive CLL compared to normal B cells, with $\Delta\Delta$Ct of 6.7 and 4.1, respectively (Supplemental Table S1.). Subsequent studies showed that targeting these receptors with their respective ligands, VIP and ACTH, raised cAMP in CLL cells (data not shown). In CLL cells from 3 patients, treatment with VIP alone and IR284 alone or the combination of IR284 with VIP or ACTH increased apoptosis in aggressive CLL compared to untreated cells, while IR284 treatment increased apoptosis in indolent CLL cells. Because these data were generated with samples from a small number of patients, I sought to expand the data set with two additional patients with each disease subtype.

3.2.1: ACTH or VIP in combination with IR284 induce apoptosis in CLL cells

When additional patient samples were incorporated into this data set (n_{total}=5), an overall reduction of the mean level of drug-induced apoptosis was observed in aggressive CLL. In contrast to previous data (n=3), aggressive CLL

cells treated with VIP displayed a non-significant increase in apoptosis (14.85 ± 6.26%, $p > 0.05$) compared to untreated CLL cells. However, VIP in combination with IR284 significantly increased apoptosis (29.1 ± 9.06%, $p < 0.05$) versus untreated, though these values are decreased compared to the initial data (VIP alone 24.6± 3.37%, VIP+ IR284 42.7%± 6.5%). Aggressive CLL cells treated with ACTH in combination with IR284 had increased apoptosis (30.6± 9.93%), but this value is much lower than previous data had suggested (45.9 ± 6.06%). Similarly, aggressive CLL cells treated with IR284 alone had increased apoptosis compared to untreated cells, but the mean percentage of cells undergoing drug-induced apoptosis decreased from 32.6± 5.95% to 23.7 ± 6.58% when two additional patients were added to the data set (Figures 3.1 and S1). These results suggest that the mean apoptosis of aggressive CLL cells was less robust for all treatments and that treatment with VIP did not increase apoptosis in IR284-treated cells compared to IR284 treatment alone.

Consistent with the original data, indolent CLL cells generally had lower apoptotic responses to each treatment compared to aggressive CLL cells (Figures S1 and S2); however, cell death was greater than that of untreated CLL cells if the cells were treated with VIP+ IR284 (12.7± 2.4%, $p < 0.01$), ACTH with (11.7± 2.61%, $p < 0.05$) or without IR284 (3.7 ± 1.15% $p <0.05$), or IR284 alone (15.5±1.67% $p <0.05$) (Figure 3.2). Similar to the trend observed in aggressive CLL, neither ACTH nor VIP in combination with IR284 significantly increased apoptosis relative to IR284 alone.

Pooled data for both indolent and aggressive CLL (n_{total}=10) suggested that treatment with IR284 (19.6± 11.01%, $p < 0.001$), ACTH with (21.2 ± 18.3% $p < 0.01$) and without (5.7 ± 5.34% $p < 0.01$) IR284, and VIP with IR284 (21.0±16.4% $p < 0.01$) increase apoptosis compared to untreated CLL cells (Figure 3.3). I conclude that PDE inhibition was the most effective treatment in promoting apoptosis. Response to the dual treatments (VIP or ACTH + IR284) differed from treatment with either GPCR ligand alone, but neither VIP nor ACTH treatment alone increased apoptosis beyond 10%.

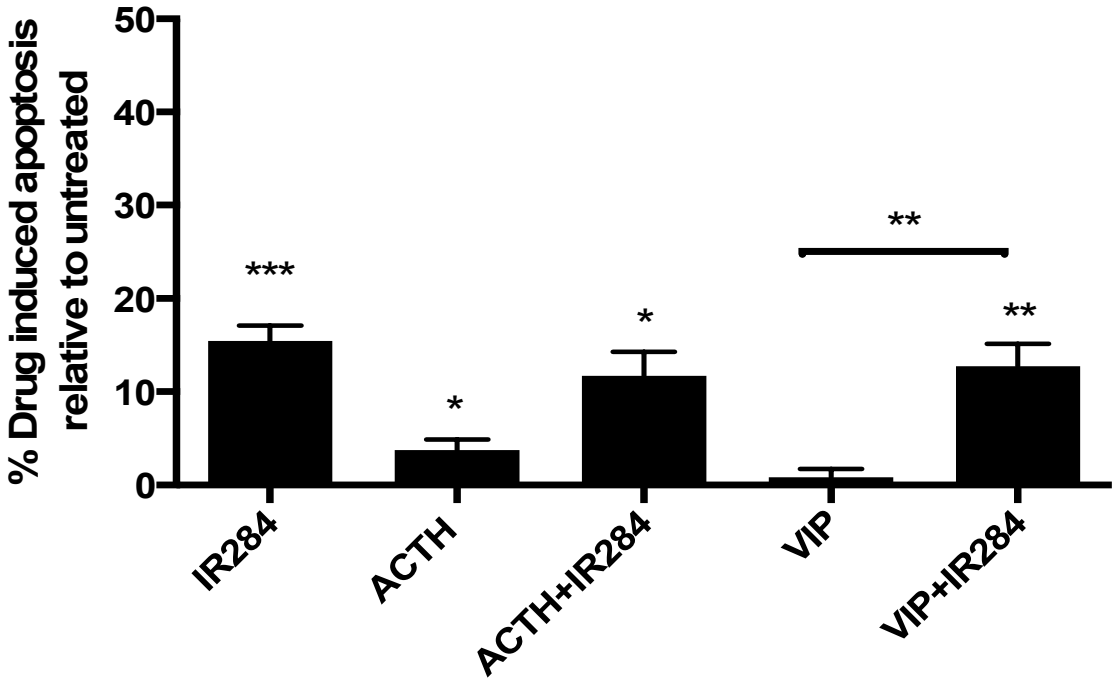

Figure 3.1 Apoptosis of indolent CLL cells (n=5) in response to treatment with 100 nM IR284 alone, 1 μM VIP or 1 nM ACTH alone or in combination with 100 nM IR284. Statistical significance determined by one-way ANOVA with Fischer's LSD post-test, and is depicted by (*) for p value < 0.05, (**) for p value < 0.01, and (***) for p value < 0.001. Each treatment is compared to the untreated group and single treatment groups (e.g. VIP) were compared to the related dual treatment (VIP + IR284). Generated in collaboration with A. Wilderman and L. Brown.

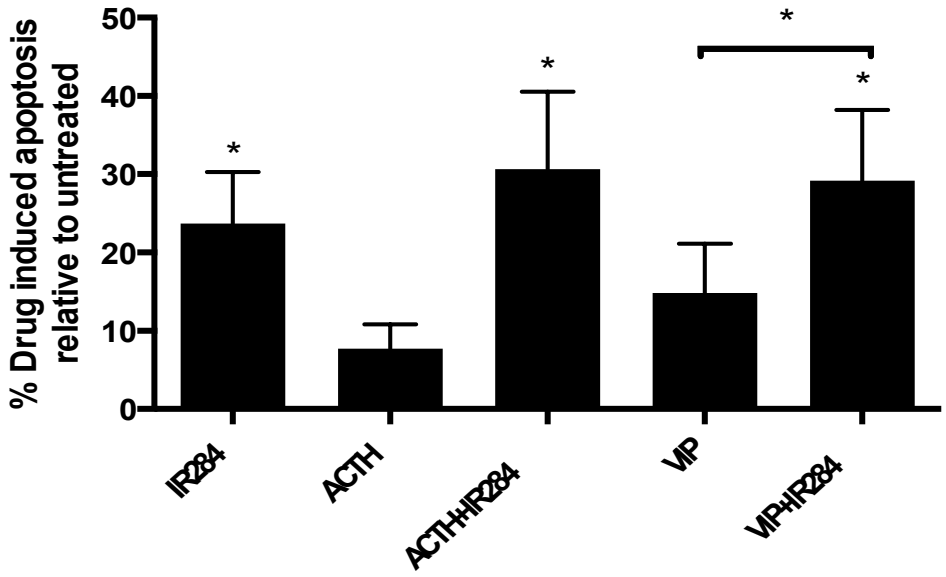

Figure 3.2 Apoptosis of aggressive CLL cells (n=5) in response to treatment with 100 nM IR284 alone, 1 μM VIP or 1 nM ACTH alone or in combination with 100 nM IR284. Statistical significance determined by one-way ANOVA with Fischer's LSD post-test, and is depicted by (*) for p value < 0.05. Each treatment is compared to the untreated group and single treatment groups (e.g. VIP) were compared to the related dual treatment (VIP + IR284). Generated in collaboration with A. Wilderman and L. Brown.

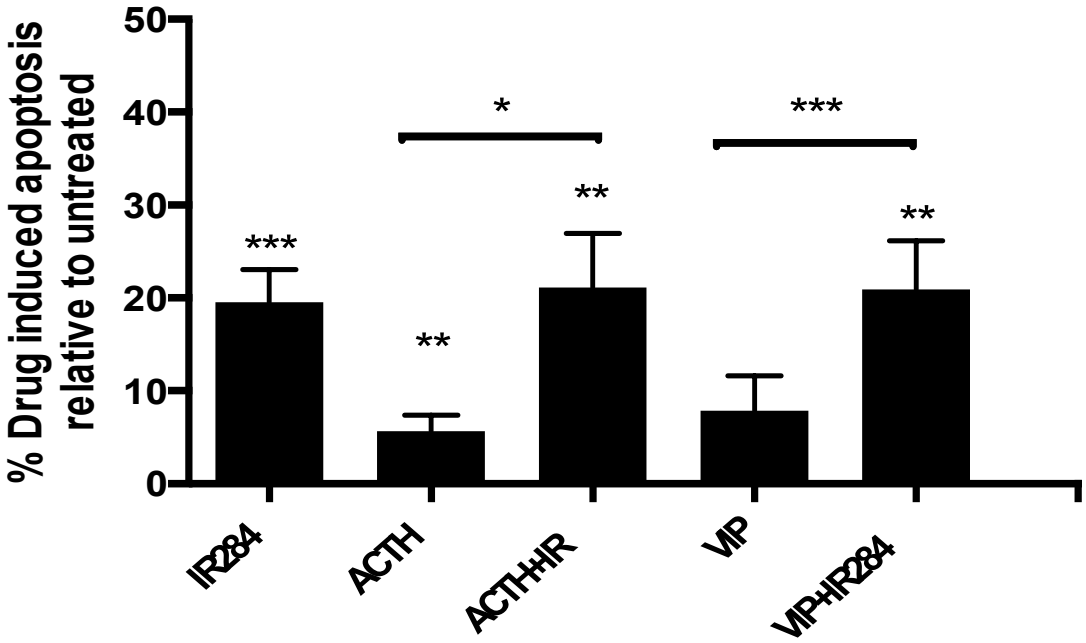

Figure 3.3 Apoptosis of indolent and aggressive CLL cells (n=10) in response to treatment with 100 nM IR284 alone, 1 μM VIP or 1 nM ACTH alone or in combination with 100 nM IR284. Statistical significance determined by one-way ANOVA with Fischer's LSD post-test, and is depicted by (*) for p value < 0.05, (**) for p value < 0.01, (***) for p value < 0.001. Each treatment is compared to the untreated group and single treatment groups (e.g. VIP) were compared to the related dual treatment (VIP + IR284). Generated in collaboration with A. Wilderman and L. Brown.

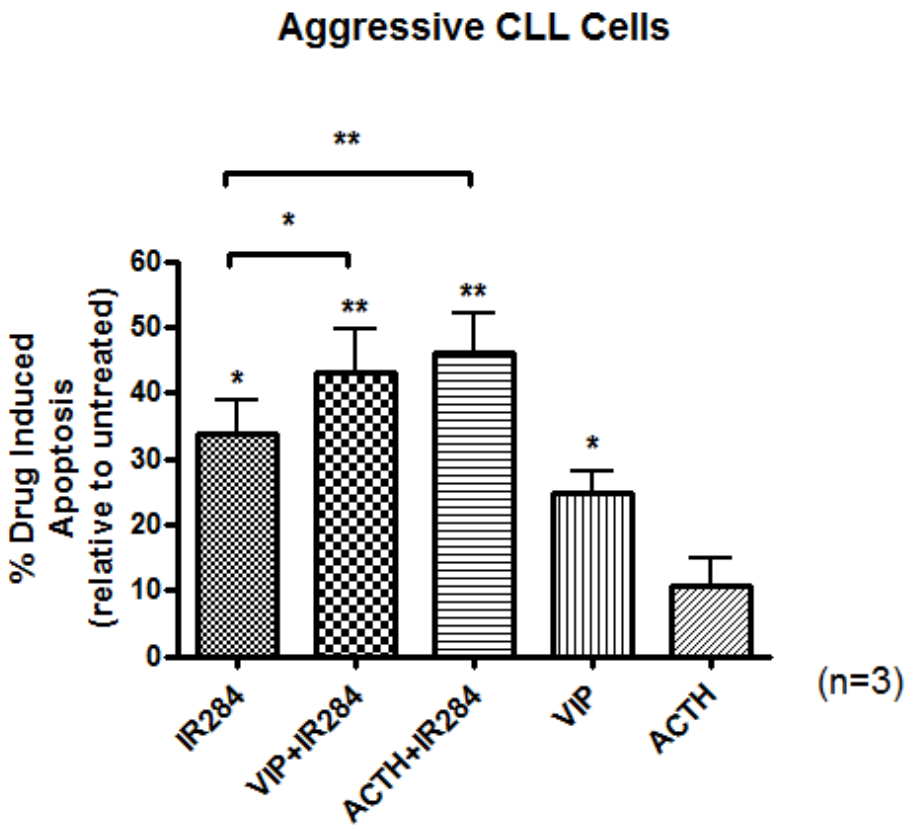

Supplemental Figure S1 Apoptosis of aggressive CLL cells (n=3) in response to 100 nM IR284, 1 μM VIP+100nM IR284, 1 nM ACTH+100nM IR-284, 1 μM VIP, and 1 nM ACTH. Statistical significance was determined by Student's t-test and is depicted by (*) for $P<0.05$ and (**) for $P<0.01$ for samples that were compared to either untreated cells and cells treated with IR284 alone. Performed by Trishna Katakia.

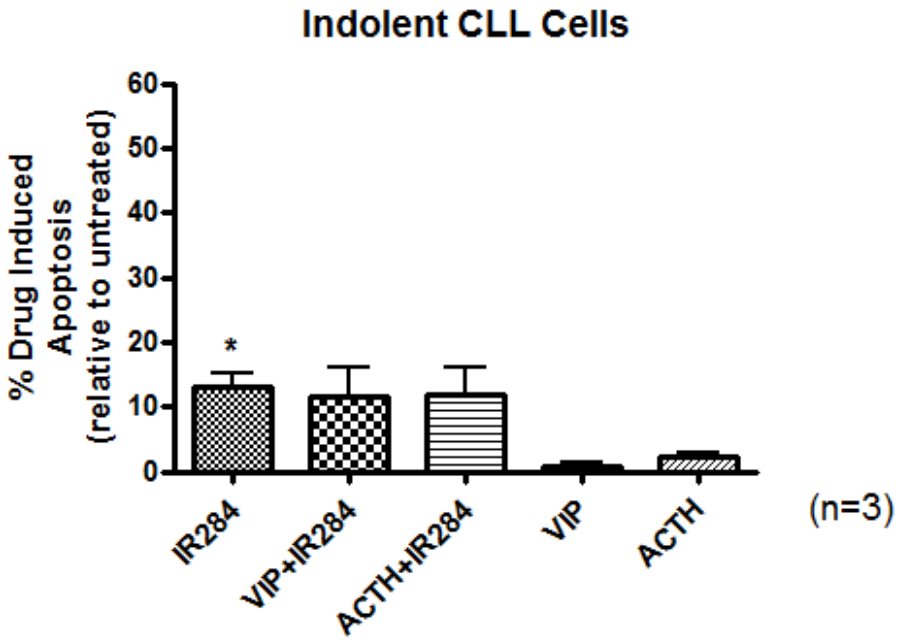

Supplemental Figure S2 Apoptosis of indolent CLL cells (n=3) in response to 100 nM IR284, 1 μM VIP+100 nM IR284, 1 nM ACTH+100 nM IR-284, 1 μM VIP, and 1 nM ACTH. Statistical significance was determined by Student's t-test and is depicted by (*) for $P<0.05$ for samples compared to untreated cells. Performed by Trishna Katakia.

Supplemental Table S1 GPCR with the greatest difference in expression (ΔΔCt values) between normal B cells, indolent CLL cells, and aggressive CLL cells. Data by Trishna Katakia

Indolent vs. Normal		Aggressive vs. Normal		Aggressive vs. Indolent	
GPCR	**ΔΔct**	**GPCR**	**ΔΔct**	**GPCR**	**ΔΔct**
EDG7 (Gi) (LPA receptor 3)	**8.0**	**VIPR1 (G_S) (vasoactive intestinal peptide)**	**4.5**	**VIPR1 (G_S) (vasoactive intestinal peptide)**	**9.5**
AGTRL1 (Gi) (angiotensin receptor-like 1)	**6.8**	**MC2R (G_S) (melanocortin 2 receptor)**	**4.1**	**P2RY14 (Gi) (purinergic receptor P2Y 14)**	**3.2**
MC2R (G_S) (melanocortin 2 receptor)	**6.7**	**Cannabinoid CB_2 (Gi)**	**3.2**	**FPRL2(Gi) (formyl peptide receptor-like 2)**	**1.6**

3.2.2 Co-culture with NKtert reduces basal apoptosis of CLL cell in vitro

Due to high basal apoptosis (as high as 75-90% by 48 hours), there was a limited dynamic range in which to observe treatment-induced CLL cell death. Resistance to apoptosis by malignant B cells characterizes CLL; therefore, this high level of basal apoptosis *in vitro* demonstrates the importance of stromal interactions in the pathology of CLL *in vivo*. We hypothesized that studying CLL in a co-culture system with stromal cells would improve the range within which to measure treatment-induced apoptosis and would more closely mimic the physiological conditions that exist *in vivo*. Therefore, to assess the most effective means by which to extend the *in vitro* lifetime of the CLL B cells, we evaluated the viability of cells that were either co-cultured with NKtert stromal cells, treated with NKtert conditioned media or incubated with a reducing agent (βME or TCEP). We observed the greatest reduction in basal apoptosis in the co-culture group compared to the untreated group (20% decrease, Figure 3.4) and a roughly 10% decrease in apoptosis in CLL cells treated with NKtert conditioned media, but no improvement in viability of CLL cells incubated with either reducing agent. These results thus indicated that NKtert cells may provide both contact-dependent and soluble elements that improve CLL cell viability, and that this pro-survival effect was not replicated by either reducing agent.

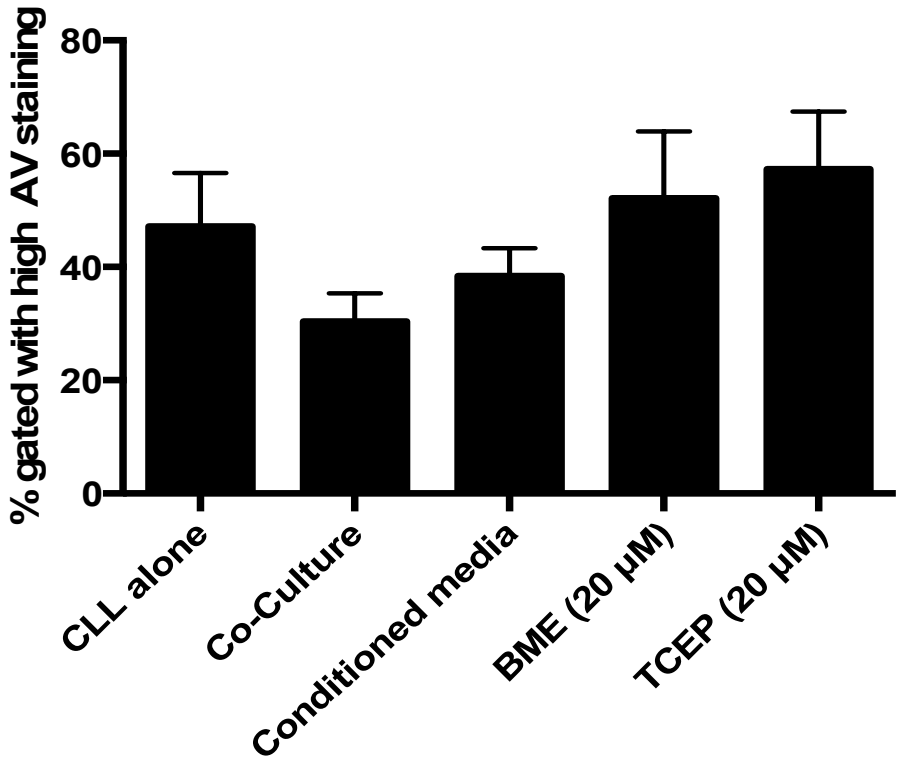

Figure 3.4 Apoptosis of CLL cells (n = 5) in direct co-culture with NKtert stromal cells (1 x 10^5), supplemented with conditioned media from NKtert or treated with βME (20 μM) or TCEP (20 μM) for 48 hours. Generated in collaboration with A. Wilderman.

3.3 Results part II: Characterization of NKtert stromal cells

3.3.1 Quantification of GPCR expression in NKtert stromal cells

To define the GPCR expression profile of NKtert stromal cells, I used TaqMan® GPCR arrays. The 384 genes analyzed on these arrays include 31 non-GPCRs (a quadruplicate of 18S rRNA and 13 other housekeeping genes) plus 353 GPCR genes. The cycle threshold (Ct) of each gene was normalized to the 18S rRNA Ct value to give a ΔCt value; GPCRs with a ΔCt value ≤ 25 were considered to be expressed. Using this approach, I found that NKtert cells express 136 GPCRs (Figure 3.5). Utilizing the IUPHAR Database of Receptors and Ion Channels, I classified each receptor by its linkage to a G-protein α-subunit (G_s, G_i, $G_{q/11}$, or $G_{12/13}$). The 20 mostly highest expressed GPCRs included four orphan GPCRs, six that couple to G_i or G_q proteins, three frizzled, adhesion, $G_{12/13}$ -coupled receptors, and two G_s linked receptors (Table 3.1). Sorting the receptors on the basis of G-protein linkage revealed that G_s-linked GPCRs have lower expression than the other groups (Table 3.2).

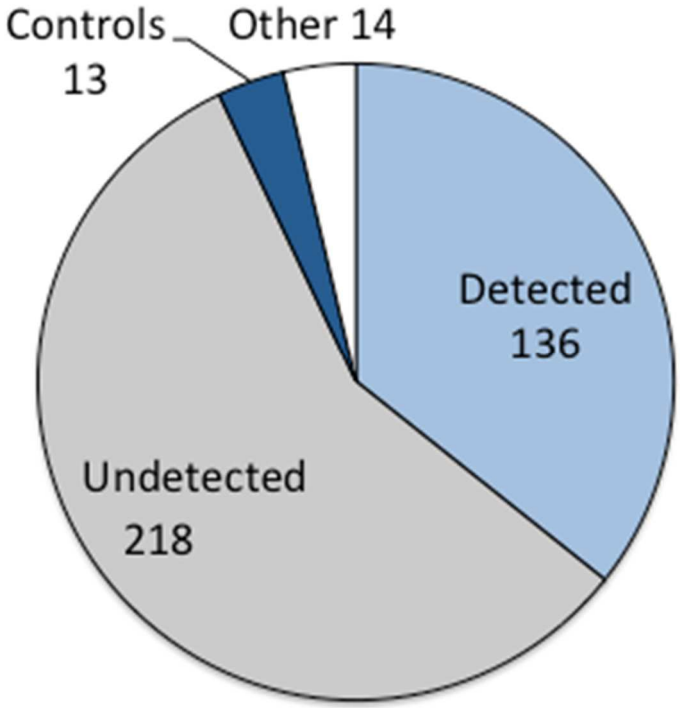

Figure 3.5 Total detected (ΔCt < 25) GPCRs in NKtert stromal cell

Table 3.1 Twenty highest detected (ΔCt < 25) GPCRs in NKtert stromal cell

Rank	Detector	Avg Ct	Avg ΔCt	Ontology
1	GPR142	10.32	0.759	Class A Orphans
2	GPR	24.47	14.92	Class A Orphans
3	FZD1	24.79	15.23	Frizzled
4	LPHN2	25.05	15.49	Adhesion Class
5	F2R	25.26	15.70	Gq/11, Gi/0, G12/13
6	CD97	25.63	16.08	G12/13 Adhesion
7	EDG2	25.858	16.30	Gs, Gq/11, G12/13
8	FZD2	26.10	16.55	Frizzled
9	OPN3	26.31	16.76	Gi/Go, Gq/G11
10	GABBR1	26.34	16.79	Gi
11	FZD4	26.43	16.87	Frizzled
12	LGR4	26.58	17.02	Class A Orphan
13	GPRC5A	26.66	17.10	Class C Orphan
14	FZD6	26.97	17.41	Frizzled
15	ELTD1	27.14	17.58	Adhesion Class
16	SSTR1	27.22	17.66	Gi/0
17	EDNRB	27.56	18.01	Gs, Gi/0, Gq/11
18	MRGPRF	27.58	18.03	Class A Orphan
19	BDKRB1	27.71	18.15	Gi/0, Gq/11
20	OXTR	27.78	18.23	Gq/11

Table 3.2 Highest expressed GPCRs on NKtert cells classified by G-protein α-subunit. GPCRs may be present in multiple categories.

Gs linkage	ΔCt	Gi linkage	ΔCt	Gq linkage	ΔCt
EDG2	16.30	F2R	15.70	F2R	15.70
EDNRB	18.01	OPN3	16.76	EDG2	16.30
GPR65	18.90	GABBR1	16.79	OPN3	16.76
PTGIR	19.19	SSTR1	17.66	EDNRB	18.01
ADRB2	20.14	EDNRB	18.01	BDKRB1	18.15

3.3.2 Quantification of PDE, PKA, and Epac-1 expression in NKtert stromal cells

There are 11 families of isoforms of cyclic nucleotide PDEs; these families are functionally distinct and exhibit unique distribution and regulatory properties[34]. PDEs hydrolyze cAMP and cGMP, making PDEs key regulators of cAMP- and cGMP-mediated signaling downstream of receptors, such as GPCRs. Previous work in the Insel laboratory showed that the PDE isoform expression profile of CLL cells is distinct from that of normal peripheral blood mononuclear cells (PBMCs)[17]. PDE7B was expressed at much higher levels in CLL cells than in normal B cells, thus implicating PDE7B as a potential therapeutic target in CLL. Since bone marrow stromal cells protect CLL cells from apoptosis, it was of interest to determine if the PDE isoform profile in stroma cells is similar to that of CLL, and if therapies targeting specific PDEs in CLL, such as the PDE4/7 dual inhibitor IR284, might also affect bone marrow stromal cells. PDE 7A was highly expressed in both CLL and NKtert cells but PDE 7B was much more highly expressed in the former. PDE4A and 4B were undetected or expressed at low levels in the stromal cells. Thus, the PDE isoform profile of NKtert cells is distinct from that of CLL cells.

Previous work performed in the Insel Laboratory by Eric Apaydin included an investigation of the mRNA expression profile of Epac-1, PKA RIIβ and RIα in CLL cells, and revealed that PKA RIα was highly expressed in PBMC (ΔCt ~ 18) and CLL-cells (ΔCt ~ 19) but that CLL cells have increased Epac-1 expression

(ΔCt ~ 20) and decreased RIIβ (ΔCt ~ 22) expression compared to PBMC ($\Delta Ct_{Epac\text{-}1}$ ~27, $\Delta Ct_{RII\beta}$ ~ 19) (Figure S4). Aggressive CLL cells had higher PKA RIIβ expression than indolent CLLcells, suggesting that compared to PBMCs, CLL cells have a higher RIα/RIIβ ratio. I thus investigated the expression profile of Epac-1 and PKA RIIβ and RIα in NKtert stromal cells and found that NKtert cells have higher expression of PKA RIα (ΔCt = 8.7), PKA RIIβ (ΔCt = 15.88), and Epac-1 (ΔCt = 16.67) than do CLL cells or normal PBMCs (Figure 3.7).

If the mRNA levels observed for PKA and Epac1 correlate with the levels of proteins expressed, the results suggest that NKtert express more of the cAMP-signaling components than do CLL cells; therefore NKtert cells may have an augmented response to agents that stimulate cAMP accumulation.

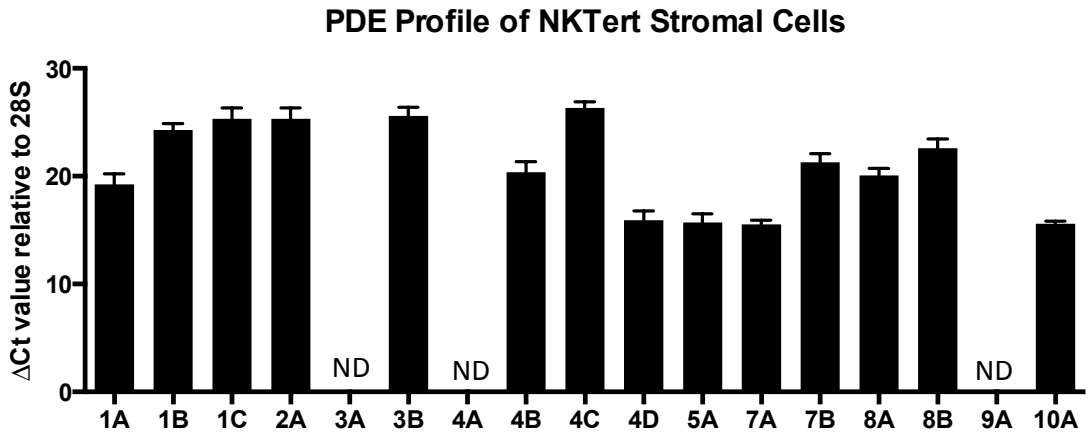

ND = Not detected before 40 cycles of qPCR

Figure 3.6a Real-time qPCR data for PDE isoform mRNA expression profile in NKtert Stromal cells

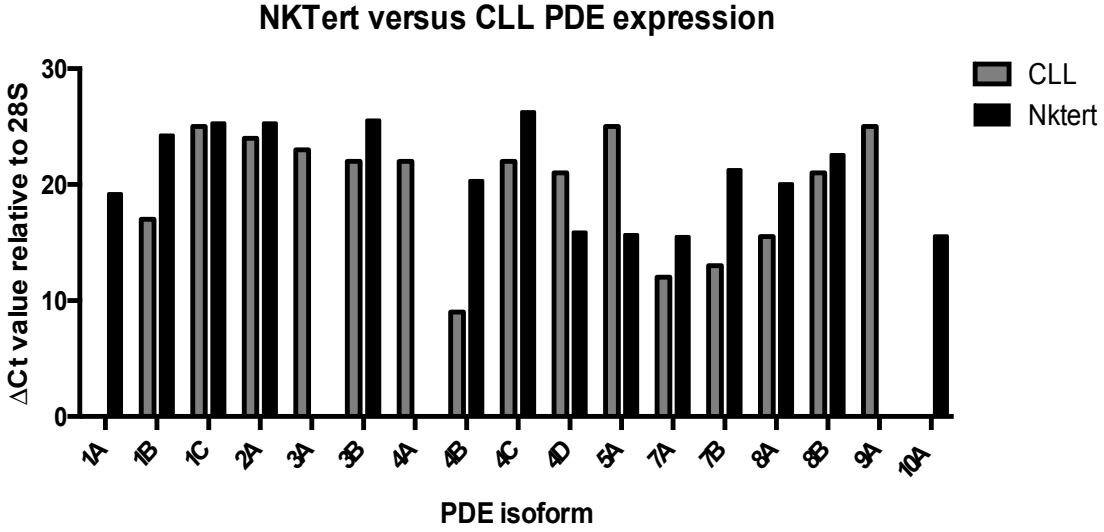

Figure 3.6b Real-time qPCR PDE isoform expression profile of NKtert Stromal cells compared to that of CLL cells, adapted from Zhang, et al 2008.

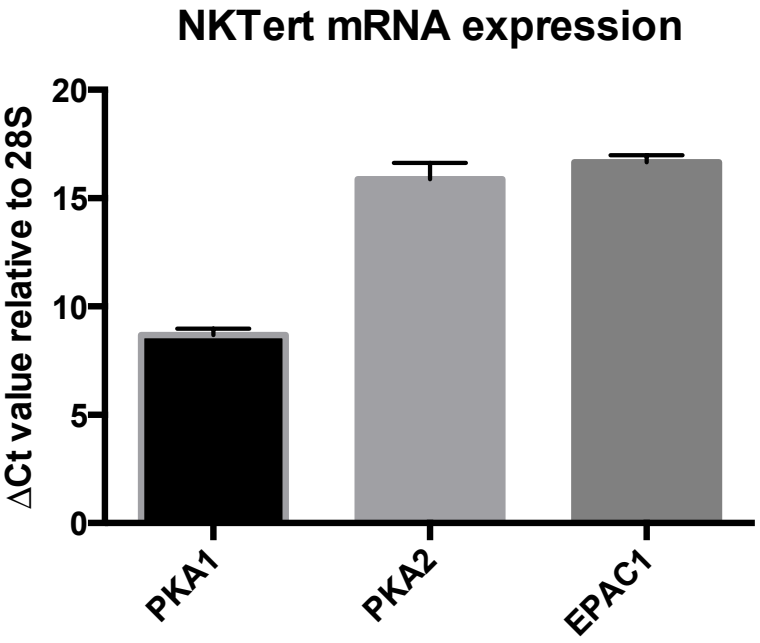

Figure 3.7 Real-time qPCR analysis of two PKA regulatory subunit isoforms (R1α and R2β) and Epac-1 mRNA in NKTert stromal cells

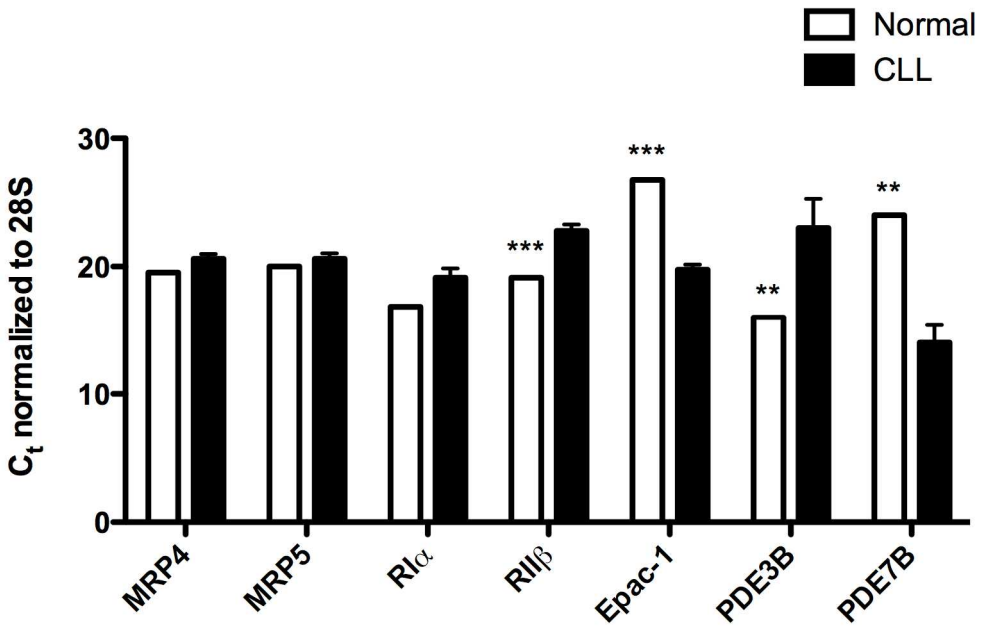

Supplemental Figure S4 Cycle thresholds (lower value denotes higher expression) normalized to 28S for MRP4 (n=33), MRP5 (n=31), RIα (n=33), RIIβ (n=22), Epac-1 (n=38, C_t values for two outliers were excluded: 14.9 and 14.6), PDE3B (n=33), PDE7B (n=56) in from CLL-cells and normal PBMC (n=12 for Epac-1, n=14 for all others), as measured by real-time PCR. Significance determined by Student's t-test is depicted by (*) for P<0.05, (**) for P<0.01, and (***) for P<0.001 compared to normal. Performed by Eric Apaydin

3.3.3 cAMP associated effects on NKtert viability and DNA synthesis

Because Epac-1 and both PKA isoforms were highly expressed in NKtert cells, I hypothesized that cAMP signaling would affect the viability or proliferation of NKtert stromal cells. The results in Figure 3.8 suggest that treatment with 50 μM 8Me, a Epac-specific cAMP analog, and both low (10 μM) and high (50 μM) concentration of N6, a PKA-specific cAMP analog, reduced the viability of NKtert stromal cells. This indicates that treatments that increase cAMP, and ultimately the activity of PKA or Epac-1 may increase apoptosis of bone marrow stromal cells. However, Figure 3.9 indicates that [^{3}H}thymidine incorporation in NKtert cells is significantly decreased by treatment with 8Me but not N6, suggesting that Epac-, but not PKA-, mediated cAMP effects regulate DNA synthesis of the NKTert cells. IR284, VIP and ACTH did not alter [^{3}H]thymidine incorporation of NKtert cells.

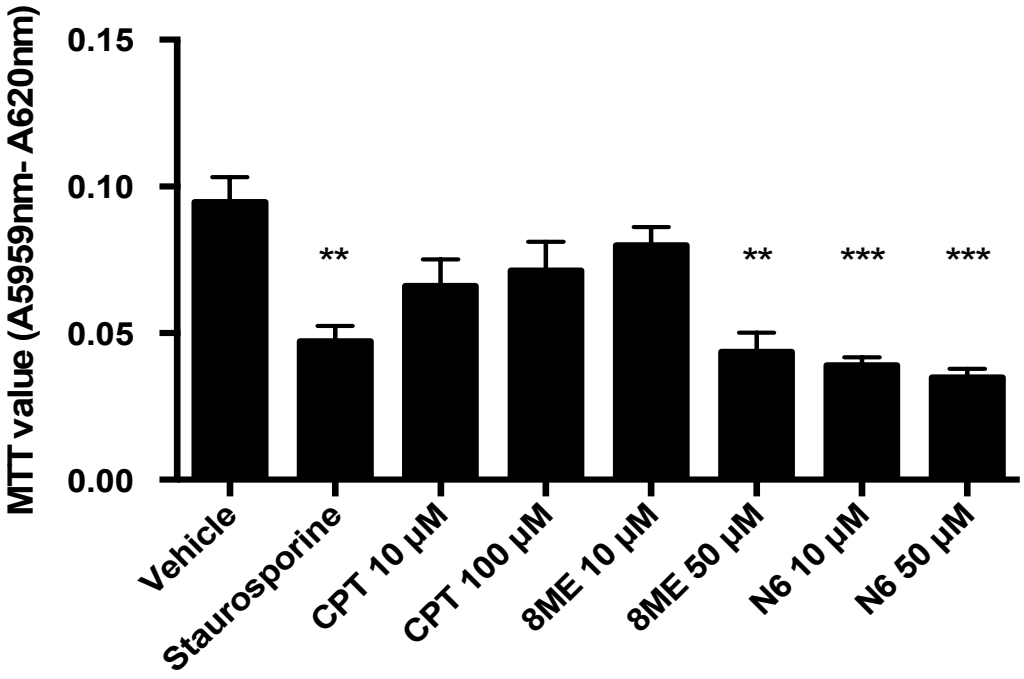

Figure 3.8 Viability of NKtert stromal cells treated with various cAMP analogs (CPT, N6, 8Me) and staurosporine related to untreated control

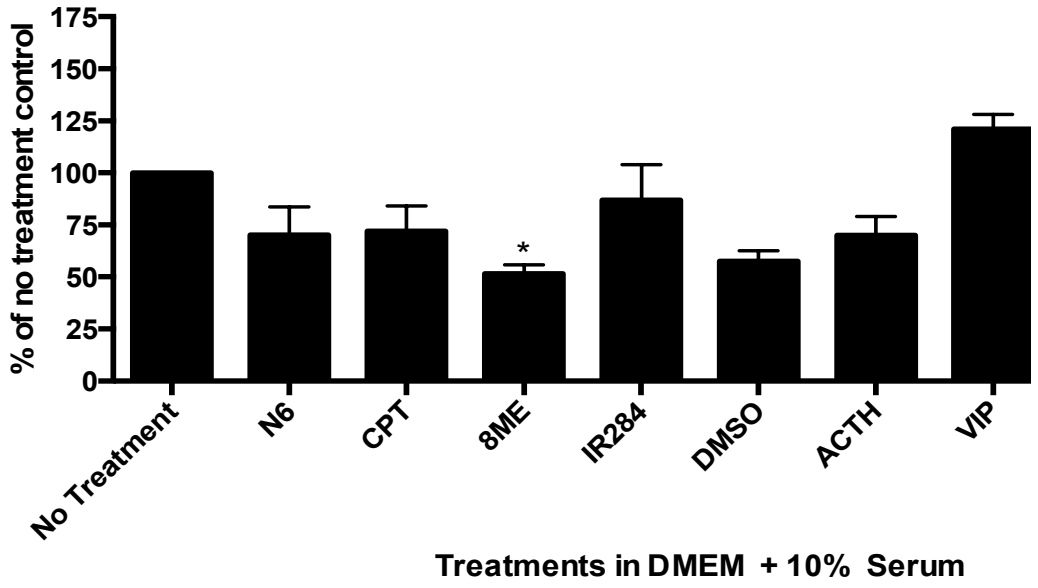

Figure 3.9 [^{3}H]thymidine incorporation of NKTert cells with cAMP analog treatments (N6, CPT, 8Me 50 μM), PDE inhibitor IR284 (100 nM), ACTH (1 nM), VIP (1 μM) or vehicle DMSO.

3.3.4 Effects of CLL-secreted factors on NKtert DNA synthesis

As part of our interest in studying the bidirectional interactions between malignant CLL cells and NKtert cells, we investigated whether there were factors in the conditioned media of CLL cells that would affect NKtert DNA synthesis of NKtert cells. We found that conditioned media from cultures of normal B-cells, CLL cell lines (I83, WAC3) or CLL patients had diverse effects on [3H]thymidine incorporation of NKtert cells. Conditioned media from two different aggressive CLL patient samples had minimal effect on NKtert [^{3}H]thymidine incorporation but on average, conditioned media from indolent CLL cell cultures increased DNA synthesis by 50%. Conditioned media from the Epstein-Barr transformed CLL cell lines, I83 and WAC3, had minimal effect on NKtert DNA synthesis (Figure 3.10a). Treating NKtert cells with conditioned media from indolent CLL patient cells incubated with IR28 (100 nM) or VIP (1 μM) (as described in Figures 3.1-3.3) substantially (~65%) decreased [^{3}H]thymidine incorporation compared to conditioned media alone (Figure 3.10b). These results suggest that cAMP-stimulation of CLL cells may alter production of factors that regulate the proliferation of NKtert bone marrow stromal cells.

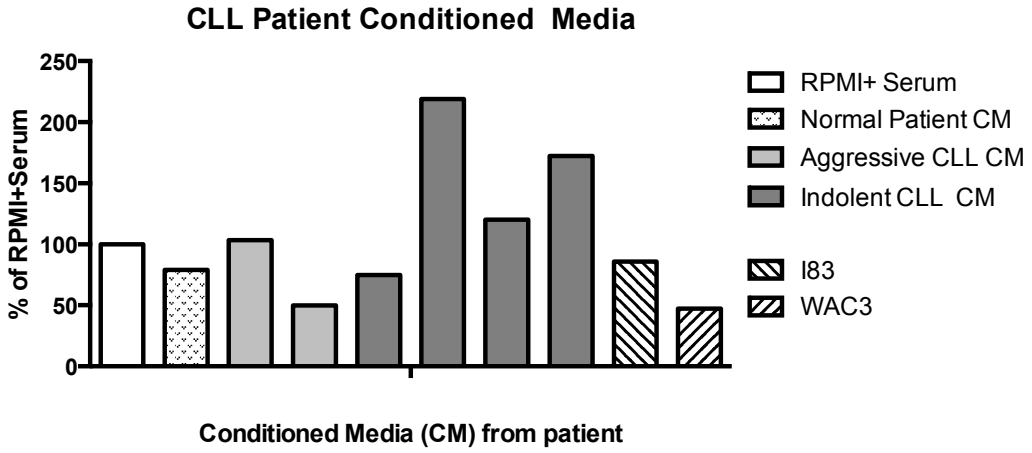

Figure 3.10a [^{3}H]thymidine incorporation of NKtert stromal cells cultured with conditioned media from Normal B-cells, Aggressive, or Indolent CLL patients or two CLL model cell lines (I83 or WAC3) for 48 hours.

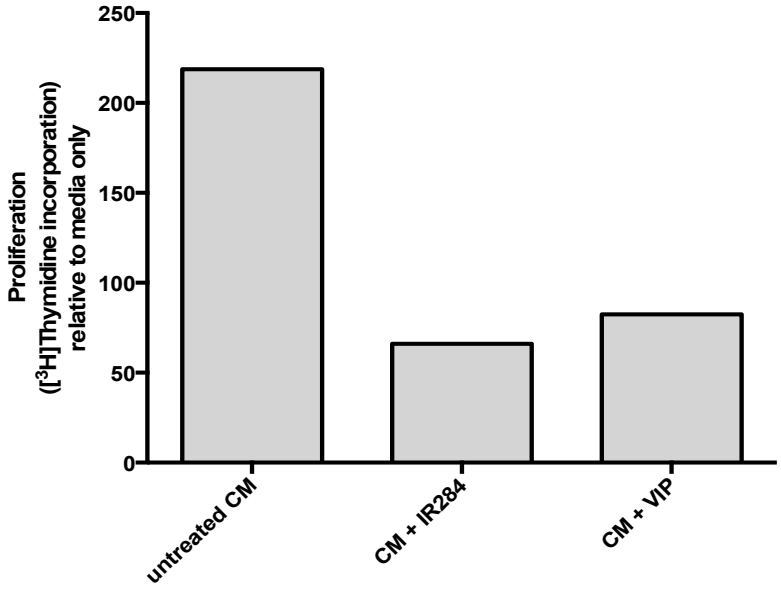

Figure 3.10b NKtert [^{3}H]thymidine incorporation when cultured in conditioned media from Indolent CLL (n=2) untreated patient cells, or indolent CLL patient cells were treated with IR284 (100 nM) or VIP (1 μM) for 48 hours prior.

3.4 Discussion

Although CLL is the most common adult leukemia in the Western world, it remains a poorly understood disease[29]. Previous Insel Laboratory member, Trishna Katakia, used TaqMan® GPCR arrays as an unbiased tool to determine GPCRs expressed in indolent and aggressive CLL cells compared to normal B cells. This work focused on GPCRs that were known to regulate intracellular cAMP levels, specifically those with G_s linkage, because cAMP induces apoptosis in CLL cells[36]. This facilitated the discovery of two putative GPCR targets, VIPR1 and MC2R. VIPR1 was significantly higher in aggressive CLL compared to indolent CLL (706-fold) and normal cells (22-fold), and MC2R was higher expressed in both indolent (110-fold) and aggressive (6-fold) CLL cells compared to normal B cells (Supplemental Table S1). VIP (vasoactive intestinal peptide) treatment increased cAMP in both aggressive and indolent CLL and induced apoptosis in aggressive CLL cells. ACTH (adrenocorticotropic hormone) treatment in combination with the PDE inhibitor IR284 increased apoptosis in aggressive CLL. Previous data generated by Trishna Katakia suggested that ACTH alone did not have a significant apoptotic effect on either aggressive or indolent CLL cells, but did increase cAMP in indolent CLL cells.

When the sample population was expanded for this analysis, I found a general trend of less drug-induced apoptosis in aggressive CLL cells (by approximately 10%) when compared to the original data (Figure 3.1 and Supplementary Figure S1). A key problem is the very high levels of basal

apoptosis in the two additional aggressive CLL cells analyzed (91% and 79%), thus lowering the dynamic range of response. The resulting effect diminishes statistically significant enhancement of apoptosis by ACTH and VIP added to IR284 treatment alone although, both GPCR agonists in combination with IR284 increased CLL cell death compared to untreated cells.

The addition of two patients to the data pool for indolent CLL cells revealed that treatment with ACTH alone and in combination with IR284, as well as dual VIP + IR284 yielded higher cell death responses than that of untreated cells. This result substantiates the finding that MC2R stimulation, which previous colleagues had shown to increase intracellular cAMP and induce cell death of indolent CLL cells. However, neither VIP nor ACTH when used in combination with IR284 increased apoptosis compared to treatment with IR284 alone. Pooling the data from indolent and aggressive CLL cells revealed that incubation with ACTH or VIP along with IR284 increased apoptosis compared to untreated CLL cells. Overall, these data suggest that targeting of Gs-linked GPCRs might promote cAMP-induced apoptosis in CLL, particularly if combined with a PDE inhibitor such as IR284. However, more definitive conclusions will require studies in samples from additional patients.

The high basal levels of apoptosis reduce the dynamic range of measurement for drug-induced cell killing and do not accurately represent the pathophysiology of *CLL in vivo*, whereby the malignant B cells resist apoptosis,

likely as a consequence of pro-survival signals from the microenvironment, including the stroma of the bone marrow. The bone marrow has been implicated in residual minimal disease, which supports clonal expansion of CLL cells resistant to treatment [43]. Co-culturing CLL cells and bone marrow-derived stromal cells (BMSCs) provides an *in vitro* system that may reduce spontaneous CLL cell apoptosis and serve as a more accurate system to model the disease.

NKtert is a mesenchymal-derived bone marrow stromal cell line that has been immortalized by infecting primary stromal cells with a retrovirus containing the human telomerase catalytic subunit (hTERT)[46]. NKtert has been used to model the interaction of the bone marrow microenvironment in CLL[43]. It has been suggested that when co-cultured, BMSCs protect CLL cells from apoptosis by facilitating glutathione- mediated antioxidant protection[44]. For this reason, we tested whether treating CLL cells with reducing agents would provide protection from spontaneous apoptosis. We compared such agents with protection by NKtert-conditioned media or co-culture of CLL cells with NKtert cells. The results in Figure 3.4 show that co-culturing the cells has the largest protective effect; conditioned media provides some protection. This proof-of-principle experiment establishes a framework for future studies to induce apoptosis in CLL cells, and that may allow greater functional range in measurement but also serving as a closer model to the physiological conditions that exist in CLL *in vivo*.

The role of bone-marrow stromal cells in CLL has not been fully defined, nor have the intrinsic characteristics of the bone marrow cells been explored. We used GPCR arrays to define the GPCR expression profile of NKtert cells and found that these cells express a large number of GPCRs (Figure 3.5) with lower expression of G_s-linked GPCRs than of other G-protein linkages (Tables 3.1 and 3.2). The Gs-linked GPCRs of interest in CLL, VIPR1 and MC2R, were not detected in NKtert cells, suggesting that the effects of VIP or ACTH treatment would be limited to the CLL cells if tested in a co-culture system. With the knowledge of their normal GPCR expression profile, it should be possible to evaluate which GPCRs change in expression in the bone marrow stroma when co-cultured with CLL cells. Extending this work, one could assess the changes in GPCR expression on bone marrow stromal cells in patients with various clinical outcomes, which may provide insight into the GPCRs and signaling molecules responsible for CLL cell infiltration of the microenvironment; such infiltration has been shown to have prognostic value[43]

PDEs play an important role in regulating intracellular cAMP levels and the expression profile of PDEs correlates with patient outcome in CLL. Specifically, higher expression of PDE7B is associated with worse prognosis [17]. My data substantiates that IR284, a dual PDE4/7 inhibitor, increases apoptosis in CLL cells. For these reasons, I investigated the PDE expression profile of NKTert cells to better predict the effect of treatment with PDE inhibitors. I found that

PDE4A was undetected, 4C had a ΔCt around 25, 4B and 4D had higher expression, with ΔCt values around 20 and 15, respectively. PDE 7A was highly expressed (ΔCt = 15) and PDE 7B was moderately expressed (ΔCt = 22) (Figure 3.6). Overall, the PDE profile of NKtert is distinct from that of CLL.

NKtert cells highly express two isoforms of PKA (RIIβ and RIα), Epac-1, and express less PDEs that break down cAMP than do CLL cells. For this reason, I hypothesized that NKtert cells may be sensitive to therapies that increase cAMP. To the best of our knowledge, the effects of cAMP on NKtert cells have not previously been defined. Figures 3.8 and 3.9 show that treatment of NKTert cells with N6, a PKA-specific cAMP analog, induced apoptosis but did not alter DNA synthesis. Treatment of NKtert cells with 8Me, an Epac-1 specific cAMP analog, induced apoptosis at high concentrations and also decreased DNA synthesis of NKtert cells. Taken together, these data suggest that increasing cAMP may inhibit the growth of both CLL cells and NKtert stromal cells.

It has been shown that coordinated actions between the CLL cells and its microenvironment, such as bone marrow infiltration, play a role in disease progression and correlate with poorer prognosis[42,44]. Other groups have shown contact-dependent influence of CLL on bone marrow cells, in which their attachment stimulated tyrosine-kinase signaling, NKTert cell proliferation, and IL-

6 secretion[47,48]. We hypothesized that there may be CLL-secreted factors that contribute to the bi-directional interaction of NKtert and CLL cells. When NKtert cells were treated with conditioned media from CLL cells, I unexpectedly observed that indolent CLL conditioned media had a greater effect on NKtert cell DNA synthesis than did conditioned media from aggressive CLL cell cultures. This may be because aggressive CLL cells display greater infiltration of the bone marrow, where contact-dependent interactions are favored. Future work will be needed to elucidate which factors show different abundance in indolent compared to aggressive CLL conditioned media; such factors could be tested individually for their effects on NKtert cells to explain this outcome.

I sought to determine if treatment with PDE inhibitors or either of the GPCR-ligands (VIP or ACTH) affects NKtert DNA synthesis and found a substantial reduction in NKtert [^{3}H]thymidine incorporation in conditioned media from indolent CLL treated with IR284 or VIP (Figure 3.10b). This finding is important because it suggests that treatment with agents that increase cAMP and induce CLL-cell death may also help inhibit the microenvironment.

In conclusion, my results revealed that treatment withIR284 can increase CLL cell apoptosis and this action seems to be greater than the pro-apoptotic action of Gs-coupled GPCR agonists. Assessing the effect of these treatments in a co-culture system with NKtert may allow greater effects to be observed by reducing the basal apoptosis of the CLL cells *in vitro*. I characterized NKtert

stromal cells by defining their GPCR expression profile and the expression patterns of mediators of cAMP signaling, including PDEs, PKA, and EPAC. Stimulation of cAMP and the resultant signaling through Epac-1 may reduce NKtert DNA synthesis and viability, while PKA activity only appeared to reduce NKtert viability. I found that NKtert cells respond to conditioned media from indolent CLL patients by increasing DNA synthesis, and that treatment of the CLL cells with agents that increase cAMP, specifically VIP and IR284, abrogates this proliferative effect in the NKtert cells.

4. GPCRs in Pancreatic Adenocarcinoma (PDAC)

4.1 Introduction

4.1.1 Pancreatic ductal adenocarcinoma (PDAC)

It is estimated that there will be 48,960 new cases of pancreatic cancer diagnosed in 2015, with 96% deriving from the exocrine ductal epithelium, known as pancreatic ductal adenocarcinoma (PDAC)[26]. Although pancreatic cancer is only the 10th most common form of cancer, it has the lowest 5-year survival rate (6%) of all cancers reported by the American Cancer Society[49,50]. It is projected to be the second leading cause of cancer-related death in the U.S. by 2020[49].This is in part because successful clinical management of the disease is very limited. There is no effective screening tool to detect the development of pancreatic cancer, and at the time of diagnosis, most patients have locally advanced or metastatic disease[51,52]. Only 20% of patients are eligible for surgical resection, the only potential curative approach for this disease. The most common course of chemotherapy is gemcitabine-based, which only modestly improves survival, indicating a need for new therapeutic strategies[53].

PDAC tumors are characteristically large, firm, light-colored masses with poorly defined boundaries that invade and obstruct the surrounding ductal tissue[54]. Genetic sequencing has shown that alterations in multiple genes are shared in most patients: KRAS (90%), CDKN2A (90%), TP53 (75%), SMAD4 (55%)[54,51]. Initial mutations in oncogenic KRAS drive the formation of precursory pancreatic intraepithelial lesions (PanINs) that develop and accelerate towards

high-grade neoplasia, and ultimately invasive carcinomas, as genetic alterations accumulate with the loss of tumor suppressor function (such as CDKN2A and TP53)[54,55]. As PDAC develops, it elicits an exaggerated desmoplastic reaction in the surrounding microenvironment. The total volume of PDAC tumors can consist of up to 90% stroma, which is primarily composed of cancer-associated fibroblasts (CAFs) and their extracellular matrix (ECM) components[54].

4.1.2 Desmoplasia and the role of tumor microenvironment

The desmoplastic characteristics of PDAC have contributed to the difficulty in treatment of the disease and its poor clinical outcome. The tumor-associated stroma includes activated pancreatic stellate cells (PSCs), which become cancer-associated fibroblasts (CAFs) under the influence of tumor cells. These proliferative myofibroblast-like CAFs, along with immune cells and blood vessels, constitute the tumor microenvironment[56]. CAFs are stimulated to deposit ECM components such as type I and III collagen, secreted factors such as transforming growth factor-β (TGFβ), fibroblast growth factor (FGF), vascular endothelial growth factor (VEGF), and other factors that contribute to immune evasion, metastasis, proliferation and therapeutic resistance of the cancer cells[57,58,59]. Further, the large amounts of ECM disturb the interstitial pressure and compresses the local vasculature, resulting in an oxygen-deficient or hypoxic tumor microenvironment, and diminished drug delivery to tumor cells[57,60]. Treatments that aim to reprogram the stroma in combination with anti-tumor

agents may facilitate better drug delivery, tumor sensitization and ultimately, improve clinical outcome[58].

4.1.3 Hypothesis and Goals

The working hypothesis of my studies is that certain GPCRs are expressed in PDAC cells, and potentially also in CAFs, relative to their normal precursors and that such GPCRs have a functional role in PDAC. As result, these GPCRs may be exploited as novel therapeutic targets, and/or as biomarkers to aid in early detection of PDAC.

4.2 Results: Use of GPCR arrays to identify GPCRs preferentially expressed in PDAC and associated microenvironment compared to normal controls.

4.2.1 Quantification of GPCR expression in PDAC patient tumors, PDAC patient cells, PDAC model cell lines, and in a normal pancreatic ductal epithelial cell line.

We used an unbiased approach, TaqMan® GPCR arrays, to define GPCR expression in three patient derived tumors, two patient-derived cell lines (79E and 34E), two established pancreatic cancer cell lines (Aspc-1 and MiaPaCa-2) and one normal human pancreatic ductal epithelial cell line (HPDE6). Among the 384 genes analyzed on the arrays are 31 non-GPCRs (a quadruplicate of 18S rRNA and 13 other housekeeping genes) along with 353 GPCRs. The cycle threshold (Ct) values of each gene were normalized to the average of four 18S rRNA Ct values to give a ΔCt value; the expression threshold for detection of each GPCR was a ΔCt value $\leq$ 25. We found that each of three PDAC tumors expressed at least 130 GPCRs, with 73 GPCRs expressed (“shared”) among them (Figure 4.2 and 4.3). Patient-derived cells (79E and 34E) each expressed more than 130 GPCRs and shared in their expression of 119 (Figure 4.4). Model pancreatic cancer cell lines Aspc-1 and MiaPaCa-2 each expressed more than 90 GPCRs, 68 of which were shared (Figure 4.6). There were 55 mutually expressed GPCRs in the patient-derived PDAC cell lines and the model cell lines (Figure 4.7). By contrast, 134 GPCRs were detected in HPDE6, the normal human pancreatic ductal epithelial cell line.

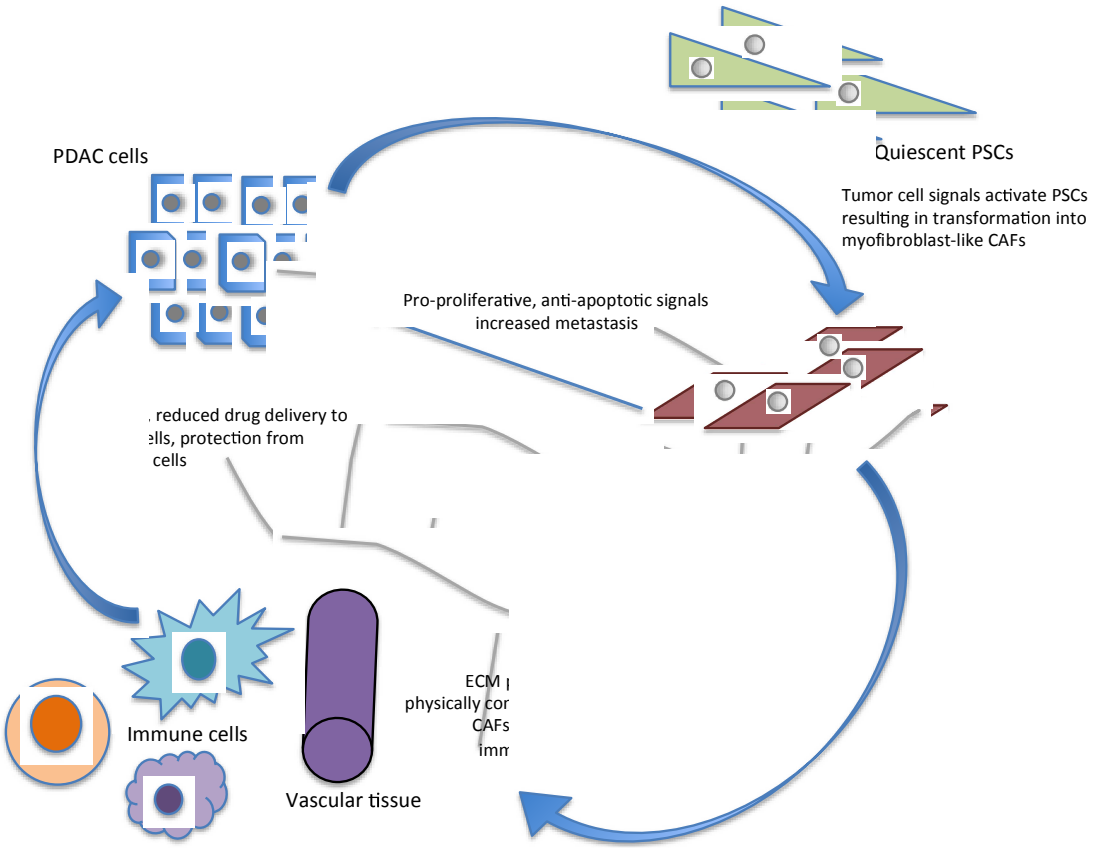

Figure 4.1 The role of microenvironment in PDAC. Signals from malignant PDAC cells activate pancreatic stellate cells (PSC) to become cancer-associated fibroblasts (CAFs), which secrete extracellular matrix components. The CAFs support tumor formation by enhancing cell proliferation, decreasing apoptosis, and reducing local immune function. The extracellular matrix which compresses the local vasculature creates hypoxia and reduces drug delivery to the tumor.

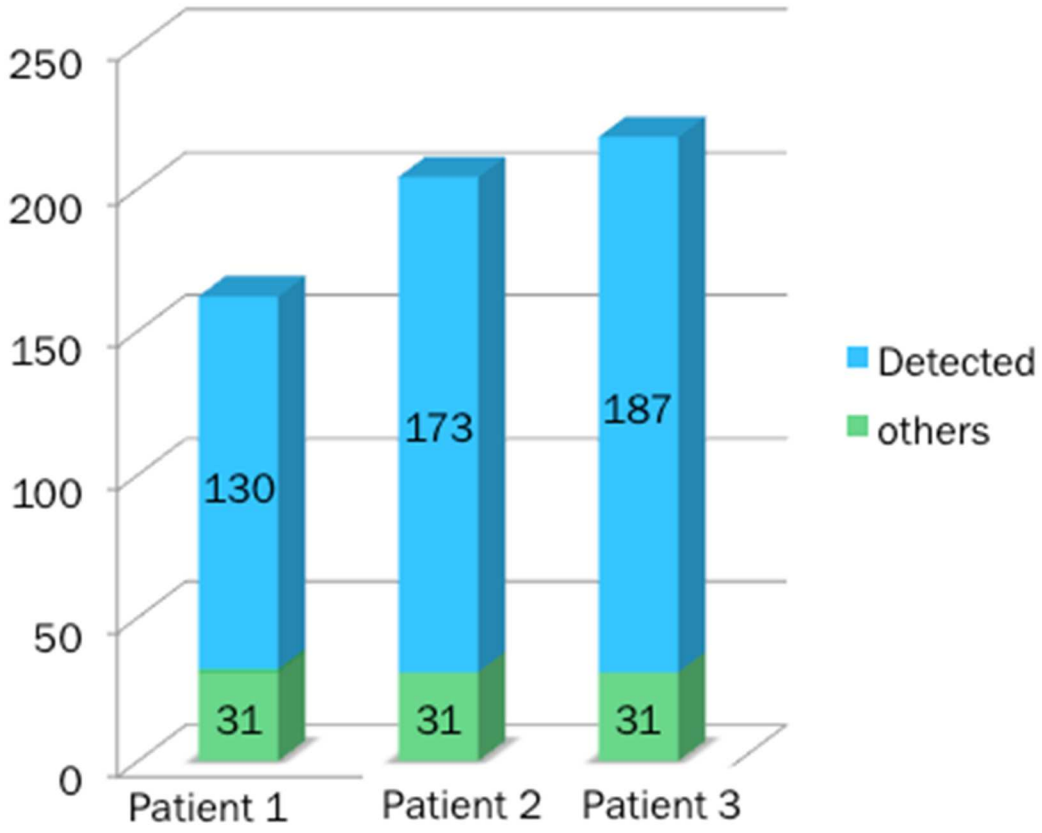

Figure 4.2 GPCRs detected in three primary PDAC tumors (ΔCt < 25)

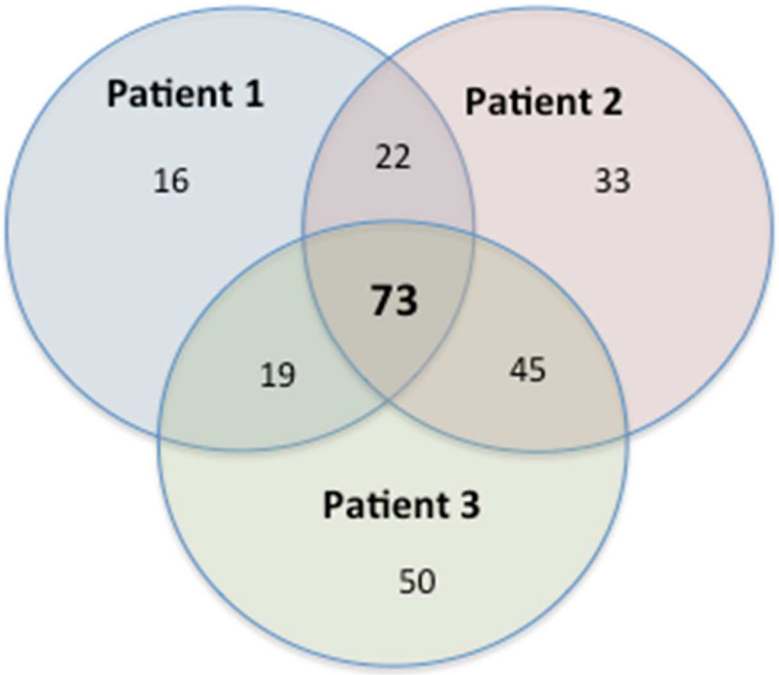

Figure 4.3 Comparison of GPCR expression between the three patient PDAC tumors (ΔCt < 25)

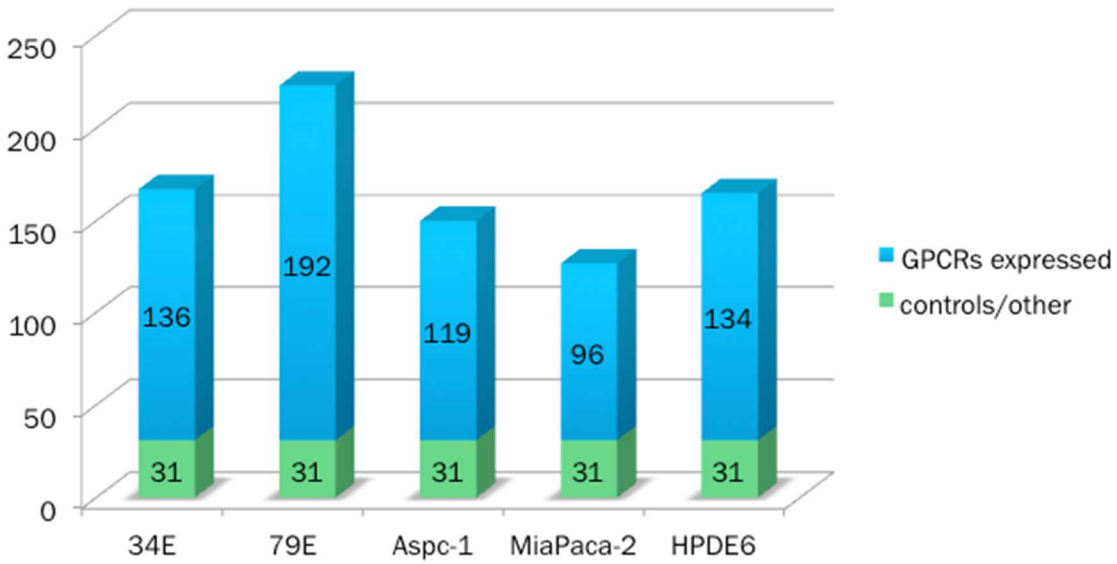

Figure 4.4 GPCR expression (ΔCt < 25) in two patient-derived cell lines (34E and 79E), two human pancreatic cancer cell lines (Aspc-1 and MiaPaca-2), and one normal cell line (HPDE6)

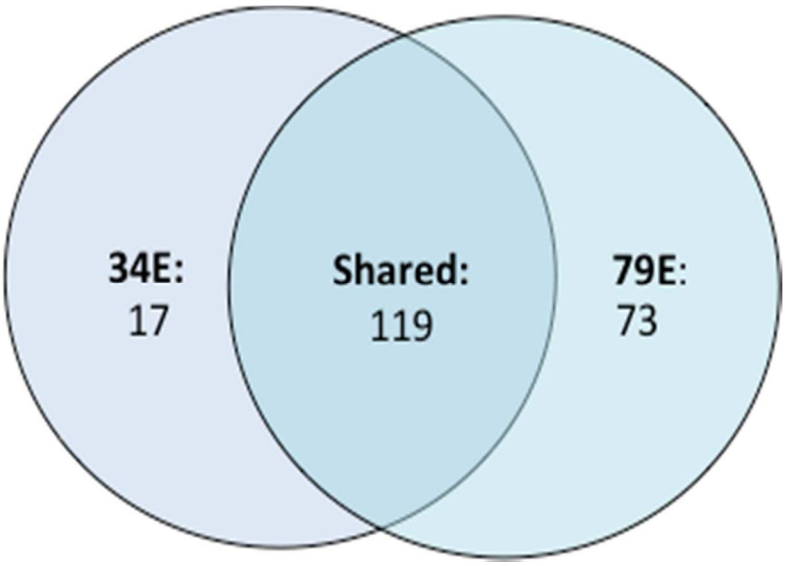

Figure 4.5 Comparison of GPCR expression in two PDAC patient-derived cell lines, 34E and 79E ($\Delta Ct < 25$)

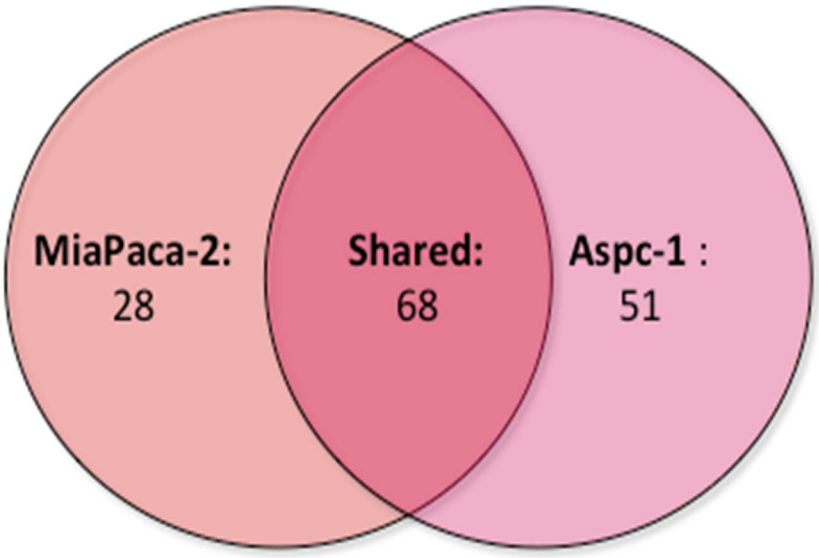

Figure 4.6 Comparison of GPCRs expressed in two established pancreatic cancer cell lines, MiaPaca-2 and Aspc-1 (ΔCt <25)

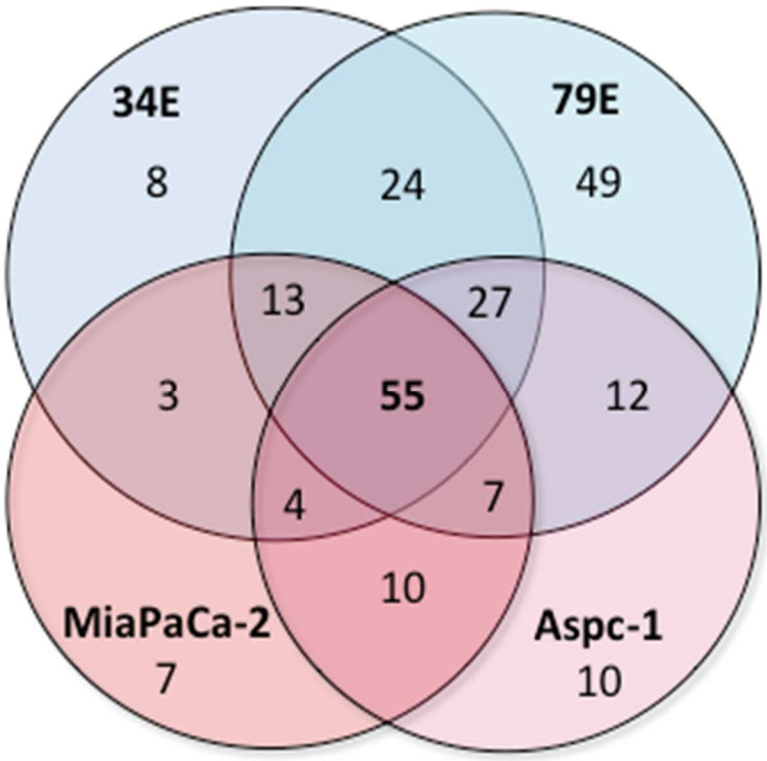

Figure 4.7 Venn diagram that compares the GPCRs expressed in two PDAC patient-derived cell lines (79E and 34E) and two established cell lines (Aspc-1 and MiaPaca-2)

4.2.2 Identification of a GPCR-of-interest, GPRC5A, in PDAC cells and pancreatic CAFs

Of the 73 shared GPCRs in the patient tumor samples, the most highly expressed was GPRC5A, with an average ΔCt value of 13.85 (Table 4.1). GPRC5A was also the highest expressed GPCR (average ΔCt value = 10.87) of the 55 GPCRs shared between the patient-derived and established cell lines (Table 4.2). Two GPCRs, GPR40 and GPR62, were detected in both patient-derived PDAC cells and both model cell lines, but not in normal HPDE6 cells and were considered "unique" to PDAC (Table 4.3). GPCRs that had a lower ΔCt value in PDAC compared to HPDE6, or a positive ΔΔCt value (where $\Delta\Delta Ct = \Delta Ct_{HPDE6} - \Delta Ct_{PDAC}$), were considered "up-regulated" or more highly expressed in PDAC. GPRC5A was one of two GPCRs that were up-regulated in 79E, 34E, Aspc-1 and MiaPaCa-2, with an average ΔΔCt value of 4.45, translating to a 21.9 fold ($2^{\Delta\Delta Ct}$) increased expression in PDAC compared to the normal cell line HPDE6 (Table 4.4). BAI1, an adhesion class GPCR, was the other GPCR that was up-regulated in the PDAC cells relative to the HPDE6 cells.

Work performed previously by my laboratory colleague Dr. Shu Zhou included TaqMan® GPCR arrays of five patient-derived pancreatic cancer-associated fibroblasts (CAFs), as well as a pancreatic stellate cells (PSCs), and normal pancreatic fibroblasts (NPFBs). PSCs and/or NPFB s are considered the precursor cells for pancreatic CAFs[61]. Dr. Zhou's data showed that GPRC5A is

the third highest expressed GPCR shared among CAF samples, with a ΔCt of 15.6 (See Supplemental Table S2). GPRC5A was one of the most highly up-regulated GPCRs compared to PSCs, with an average ΔΔCt value of 5.0, indicating 32-fold higher expression on the transformed fibroblast population compared to the precursor stellate cells (See supplemental Table S3).

Table 4.1 The 10 highest expressed GPCRS shared between three patient PDAC tumors

Gene Symbol	Ontology	Patient 1	Patient 2	Patient 3	Avg ΔCt
GPRC5A	Class C Orphan	17.73	9.85	13.98	13.85
GPR56	Gq/G11, G12/G13	16.25	12.62	16.58	15.15
CD97	G12/13 adhesion receptor	16.58	14.40	16.42	15.80
FZD5	frizzled family	17.88	13.64	17.61	16.38
VN1R1	Vomeronasal 1 Receptor 1	18.65	15.06	17.31	17.00
GPR160	Class A Orphan	16.55	16.83	18.18	17.19
C11ORF4	7TM superfamily member 1	17.33	16.20	18.17	17.23
FZD6	frizzled family	18.87	15.52	17.98	17.46
SSTR1	Gi/Go	18.08	17.36	17.10	17.51
FZD1	frizzled family	18.71	16.47	17.63	17.60

Table 4.2 The 10 highest expressed GPCRs shared between two patient-derived cell lines (34E and 79E) and two established model cell lines (ASPC-1) and MiaPaCa-2)

Rank	Gene	34E ΔCt	79E ΔCt	Aspc-1 ΔCt	MiaPaCa-2 ΔCt	Total ΔCt
1	GPRC5A	9.66	10.75	11.14	11.95	10.88
2	FZD5	14.95	13.87	14.66	17.29	15.19
3	F2R	16.77	14.66	13.96	16.75	15.54
4	CD97	16.00	16.10	14.99	15.16	15.56
5	GPR126	16.92	15.54	16.94	14.17	15.90
6	FZD6	15.77	15.16	16.07	16.82	15.95
7	OPN3	15.11	15.09	14.45	19.90	16.14
8	P2RY2	15.62	16.29	14.44	18.37	16.18
9	C11ORF4	16.11	15.75	17.04	16.19	16.27
10	GPR153	15.65	16.88	17.07	16.34	16.49

Table 4.3 GPCRs unique to both patient cell lines and established model cell lines relative to the normal pancreatic ductal cell line

Gene	Class	MiaPaCa-2 ΔCt	Aspc-1 ΔCt	34E ΔCt	79E ΔCt	Avg ΔCt
GPR40	Gq/11	23.57	22.43	24.45	22.99	24.83
GPR62	Class A Orphan	23.74	24.07	24.59	23.32	24.99

Table 4.4 GPCRs higher expressed in both patient-derived cell lines and established model cell lines relative to a normal pancreatic ductal cell line

Gene	Class	MiaPaCa-2 ΔΔCt	Aspc-1 ΔΔCt	34E ΔΔCt	79E ΔΔCt	avg ΔΔCt
BAI1	Adhesion	3.595	3.053	3.909	7.243	4.450
GPRC5A	Class C Orphan	3.346	4.147	8.107	4.537	5.034

Supplemental Table S2 Highest expressed GPCRs on CAFs, determined by Dr. Shu Zhou

Gene	Receptor name	Avg ΔCt	Signaling transduction
F2r	Protease-activated receptor 1	13.5	$G_{q/11}/G_{i/o}/G_{12/13}$
Gpr176	G protein coupled receptor 176	15.1	Class A Orphan
Gprc5a	GPCR, family C, group 5, member A	15.6	Class C Orphan
Lphn2	Latrophilin 2	15.7	Class B Orphan
Edg2	Lysophosphatidic acid receptor	15.9	$G_{q/11}/G_{i/o}/G_{12/13}$
Fzd6	Frizzled family receptor 6	16	G protein independent
Oxtr	Oxytocin receptor	16.3	$G_{q/11}$
Fzd1	Frizzled family receptor 1	16.5	canonical WNT signaling
Gpr124	G protein coupled receptor 124	16.5	Class B Orphan
Cd97	CD97 molecule	16.8	$G_{12/13}$

Supplemental Table S3 Unique and up-regulated GPCR values on CAFs relative to PSC, determined by Dr. Shu Zhou

Gene	ΔCt on PSC	ΔCt on CAFs	ΔΔCt on CAF relative to PSC
GPR40	Undetected	Undetected	N/A
GPR62	27.2	24.8	2.4
BAI1	23.4	20.3	3.1
GPRC5A	20.61	15.61	5.0

4.2.3 Validation of GPRC5A expression using real-time qPCR

Using independent qPCR to validate the Taqman® GPCR array data, I confirmed the elevation of GPRC5A expression in the three patient tumors and its up-regulation in patient-derived PDAC cells 79E and 34E, and the model cell lines Aspc-1 and MiaPaCa-2 relative to HPDE6, and in CAFs derived from the 5 different patients relative to human PSCs. Independent qPCR ΔCt values for each of these samples linearly correlated with microarray values (R^2= 0.8388, slope = 1.028) (Figures 4.8-4.11), thus providing validation for the use of the GPCR arrays.

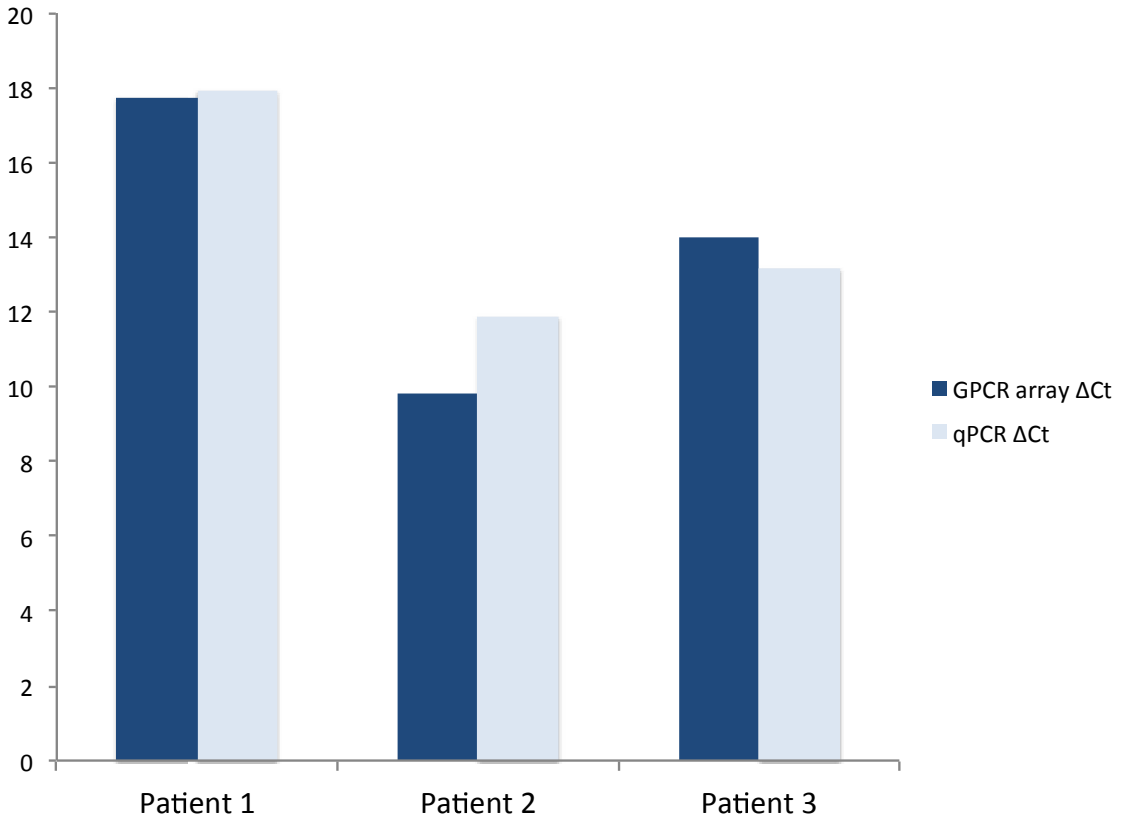

Figure 4.8 Comparison of TaqMan® and independent qPCR ΔCt values for GPRC5A mRNA expression in a three patient tumors

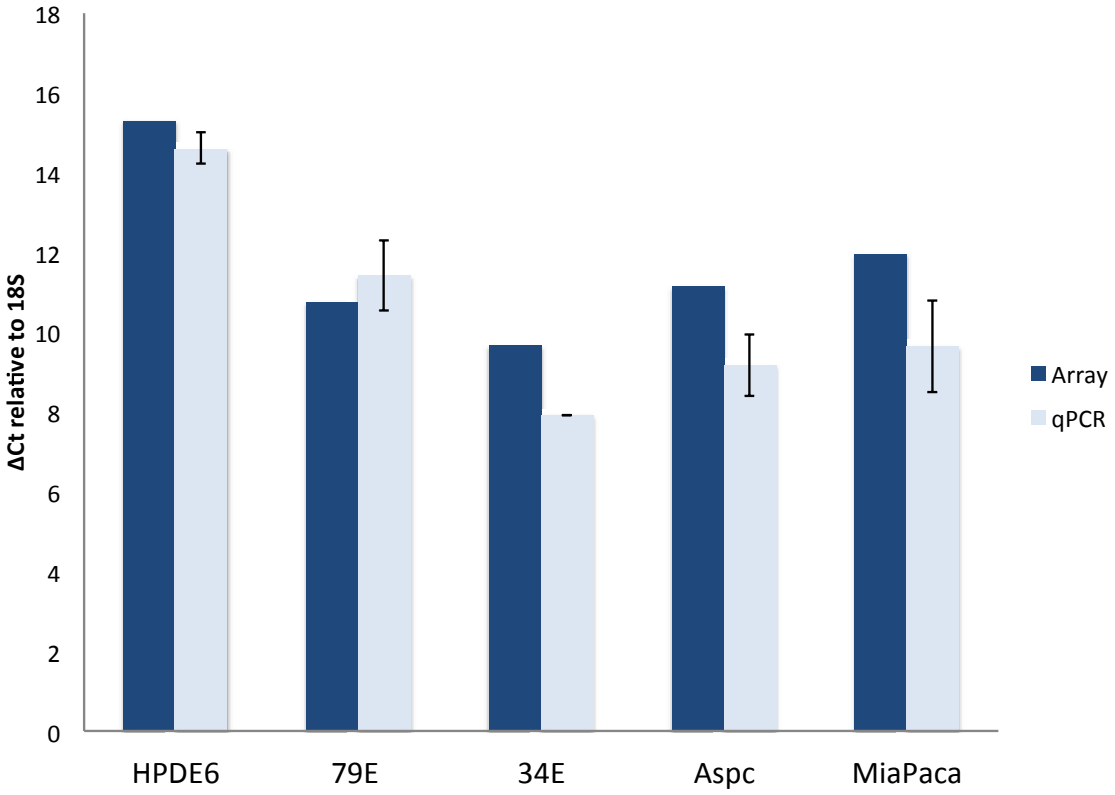

Figure 4.9 Comparison of TaqMan® and independent qPCR ΔCt values for GPRC5A mRNA expression in a normal cell line (HPDE6), two patient cell lines (79E and 34E), and two established cell lines (Aspc-1 and MiaPaca-2)

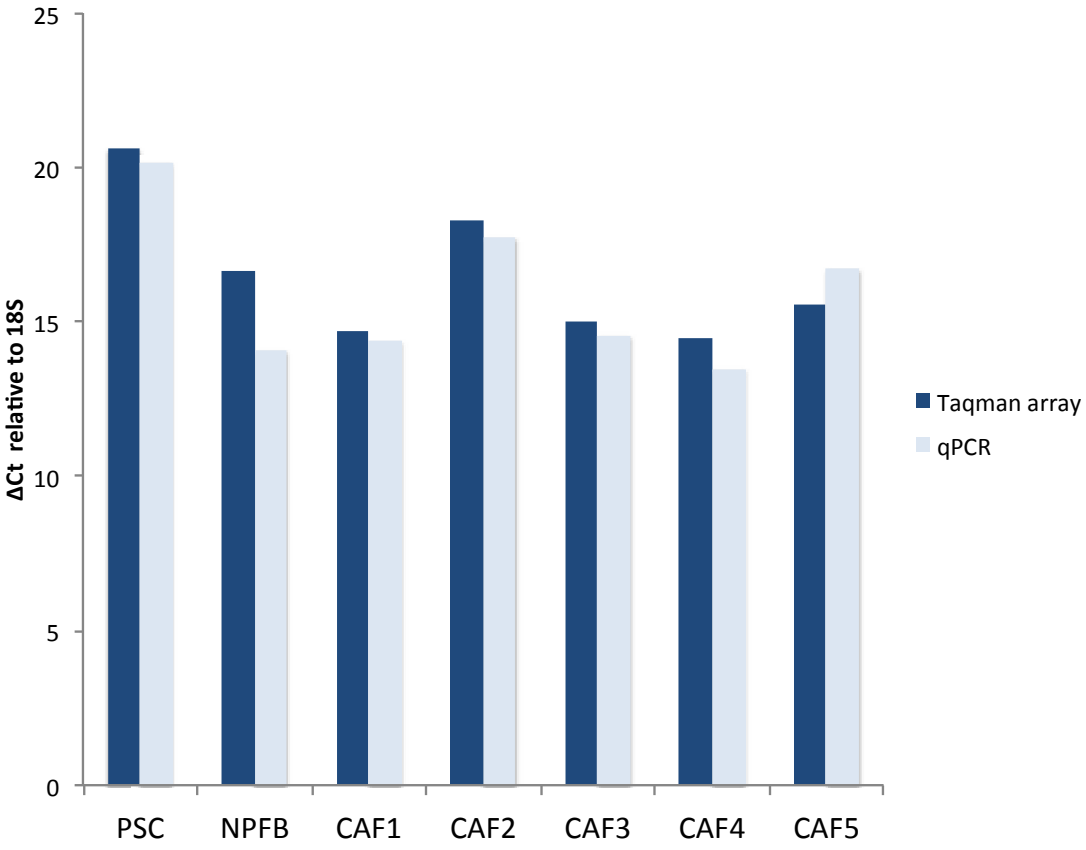

Figure 4.10 Comparison of TaqMan® and independent qPCR ΔCt values for GPRC5A mRNA expression in pancreatic stellate cells (PSCs), normal pancreatic fibroblasts (NPFB), and five patient-derived cancer associated fibroblast (CAF) samples

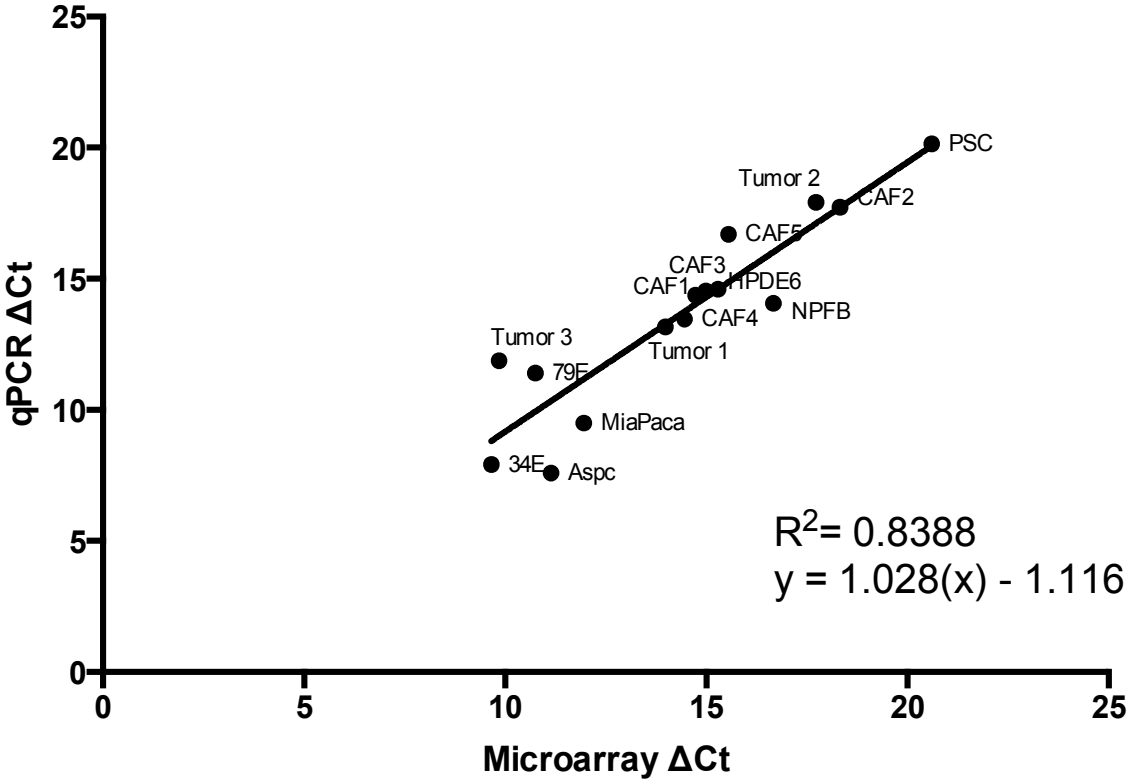

Figure 4.11 Correlation of ΔCt values for GPRC5A in PDAC tumor and cells, pancreatic CAFs, normal human pancreatic fibroblasts and normal human pancreatic stellate cells with results obtained by using either GPCR arrays or qPCR

4.2.4 Increasing GPRC5A expression increases DNA synthesis in HPDE6 cells

To assess functional activity of GPRC5A, I compared DNA synthesis in the normal cell line HPDE6 transiently transfected with a construct encoding the GPRC5a cDNA or with vector control by assessing [^{3}H]thymidine incorporation 72 hours after transfection. HPDE6 cells transfected with GPRC5A incorporated 150% more [^{3}H]-thymidine than cells transfected with an enhanced green fluorescent protein (EGFP) construct (p value = 0.0011) (Figure 4.12). Viability, assessed by intracellular ATP content, did not differ between the cells transfected with GRPC5A or control vector (assessed 48 hours after transfection, Figure 4.13). Thus, GPRC5A may stimulate PDAC cell proliferation but further studies are needed to confirm this possibility .

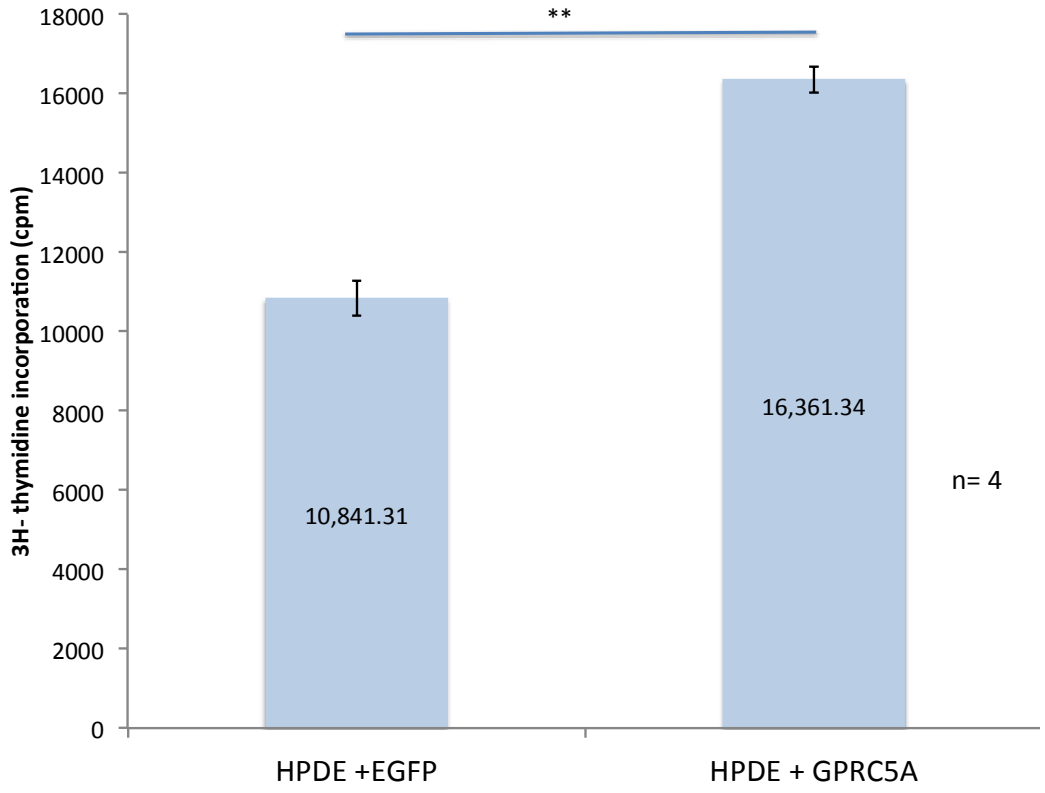

Figure 4.12 [^{3}H]Thymidine incorporation of the normal pancreatic ductal cell line (HPDE6) transfected with GPRC5A or EGFP (n=4) at 48 hours following serum addition and 72 hours after transfection

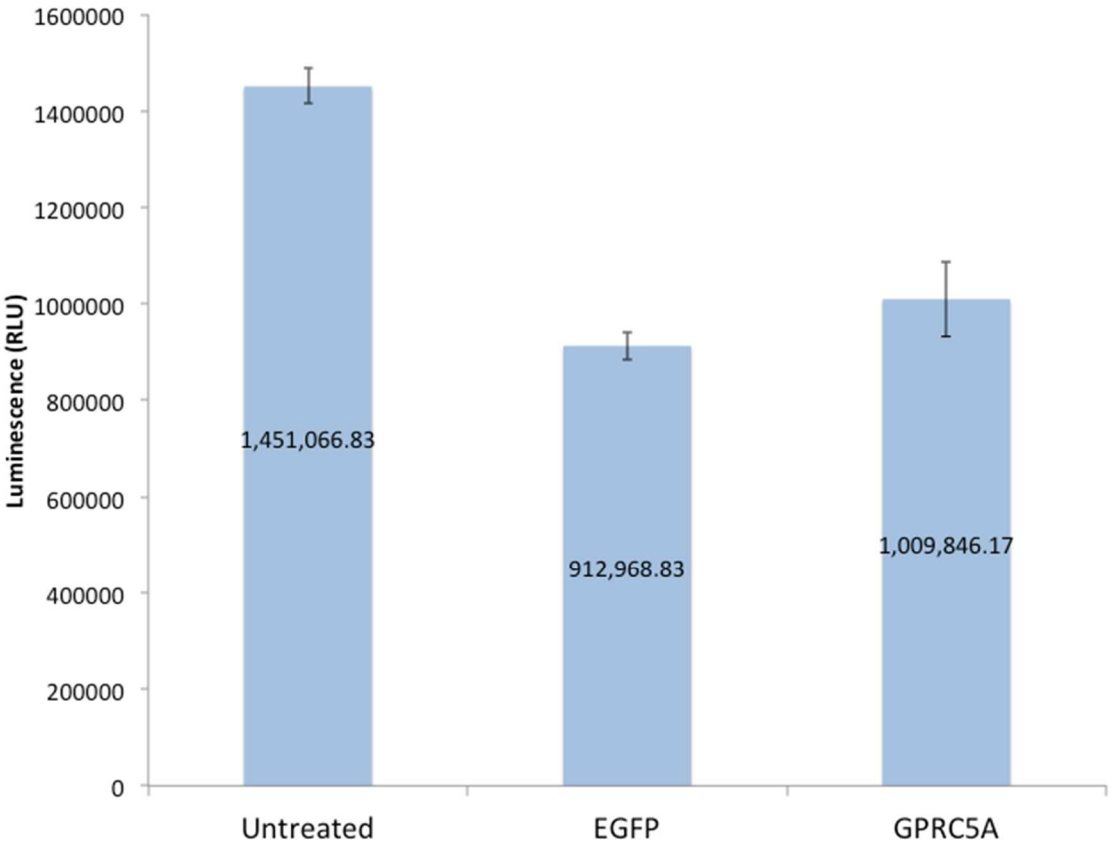

Figure 4.13 Cell-Titer Glo viability assay of untreated HPDE6 cells or cells transfected with either GPRC5A or EGFP and assessed 48 hours following transfection

4.2.5 GPRC5A tissue distribution, structural modeling, and linkage prediction

To better understand GPRC5A in PDAC tumors, I used publicly available tools to investigate its structure, function, and tissue distribution. I analyzed the structural characteristics of the receptor using I-TASSER, which employs iterative threading to assemble a predicted 3D structural model based on known templates [62]. I found that its two closest structural analogs are metabotropic glutamate receptor 1 (Figure 4.14B) and metabotropic glutamate receptor 5 (Figure 4.14C). Using Predcouple-2, I predict the G protein linkage of GPRC5A to be $G_{i,}$ (99%). The GEO profile of GPRC5A corroborates our finding that it is highly expressed in PDAC tumors relative to normal tissue (Figure 4.15). Querying the cBioPortal, I found that GPRC5A alterations exist in multiple cancer types available from the TCGA database, the highest incidence being in ovarian cancer (~9%); there is a ~3% incidence in PDAC samples (Figure 4.16). When GPRC5A copy number alterations in PDAC were plotted against mRNA expression values, GPRC5A is highly expressed in all PDAC samples shown regardless of the status of genetic alterations (Figure 4.17). This suggests that the GPRC5A expression pattern that I observed in our array data (highly expressed on PDAC relative to normal cells) mirrored publicly available data, and that this expression is not due to increased copy number or related to mutations in GPRC5A. Of note, GPRC5A expression and alterations may be important in other cancers.

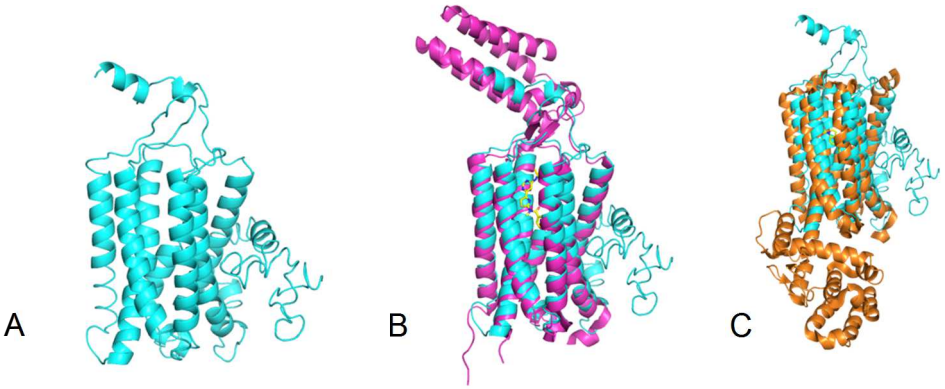

Figure 4.14 panels A-C: I-TASSER generated structural model of GPRC5A (panel A), with GPRC1A, (panel B) and GPRC1E (panel C) the first and second closest structural analogs of GPRC5A respectively.

Profile GDS4102 / 203108_at / GPRC5A

Title Pancreatic Tumor and Normal tissue samples

Organism Homo sapiens

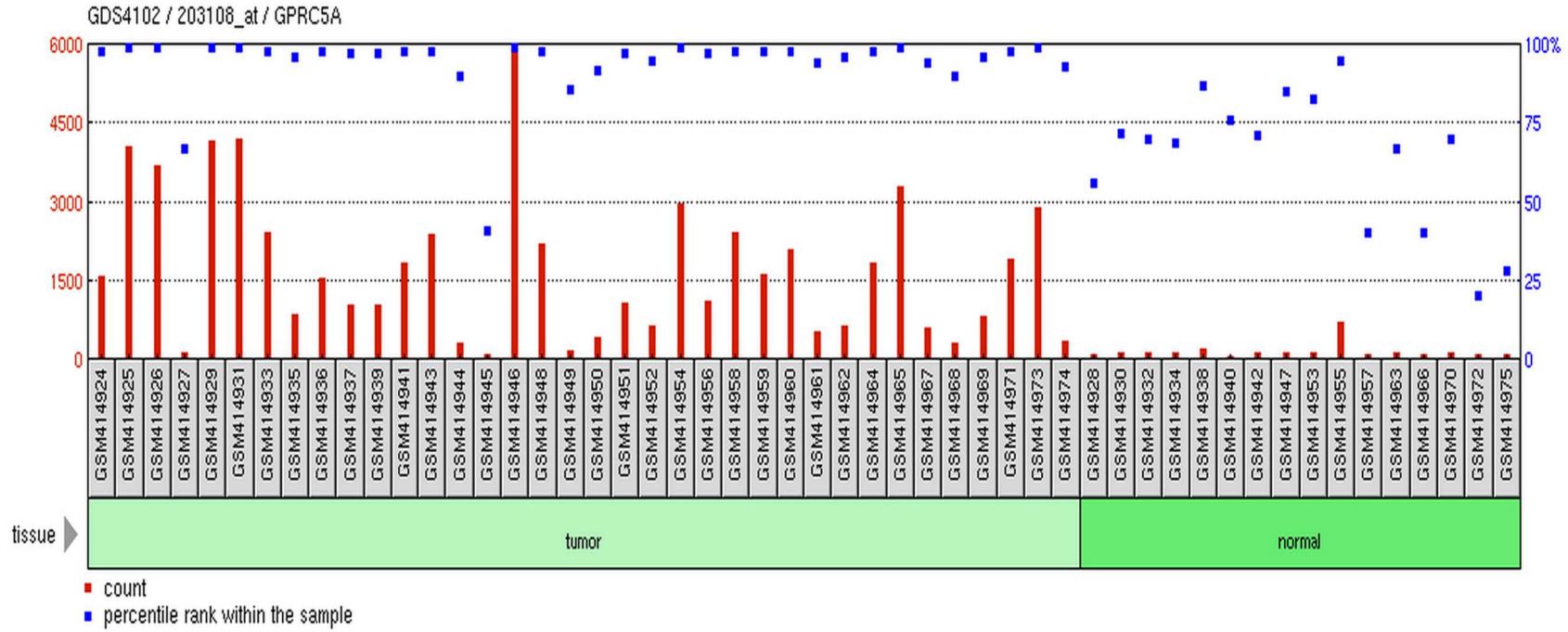

Figure 4.15 GEO expression profile of GPRC5A expression in PDAC tumor versus normal pancreatic tissue

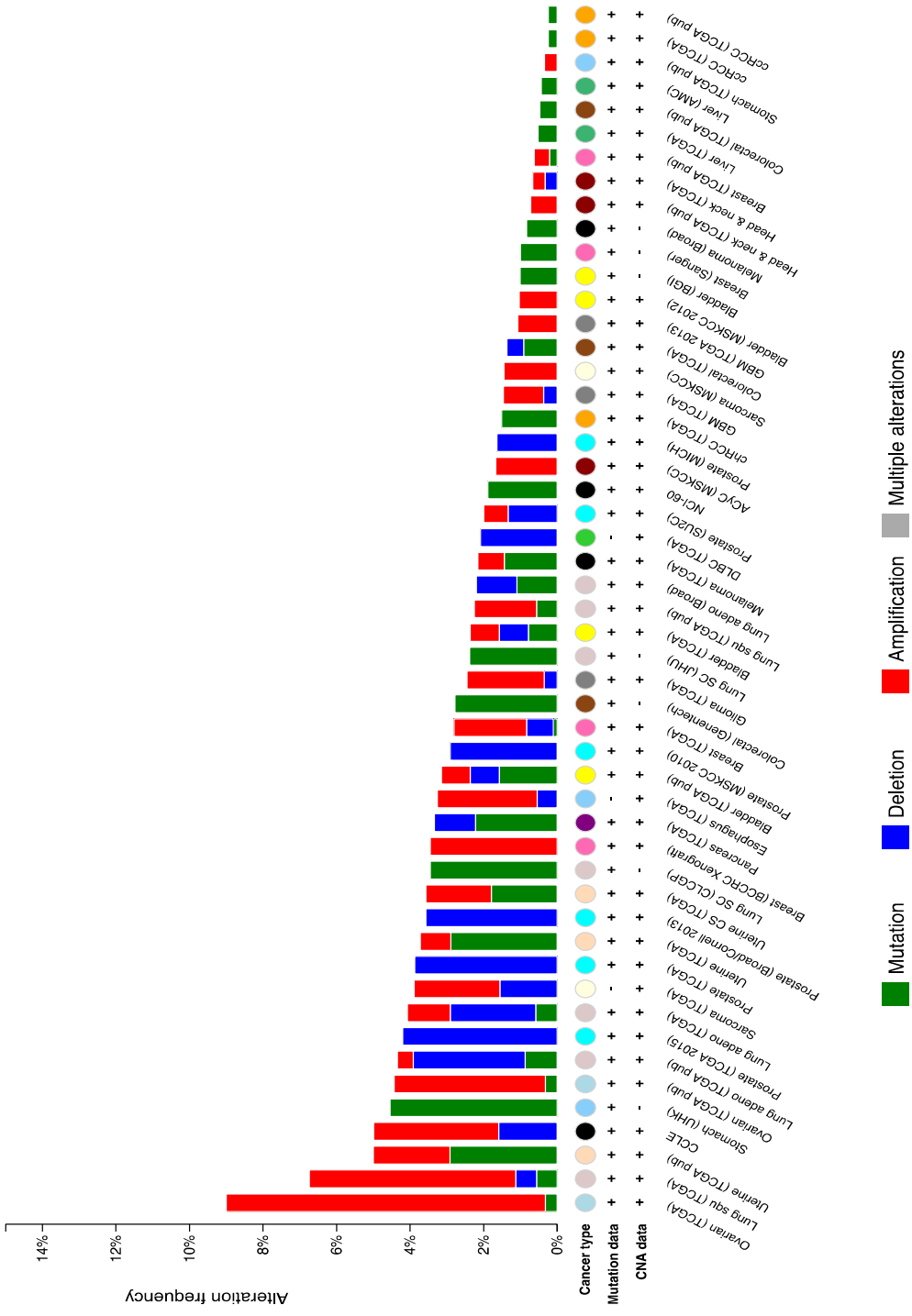

Figure 4.16 GPRC5A alterations across cancer samples from TCGA

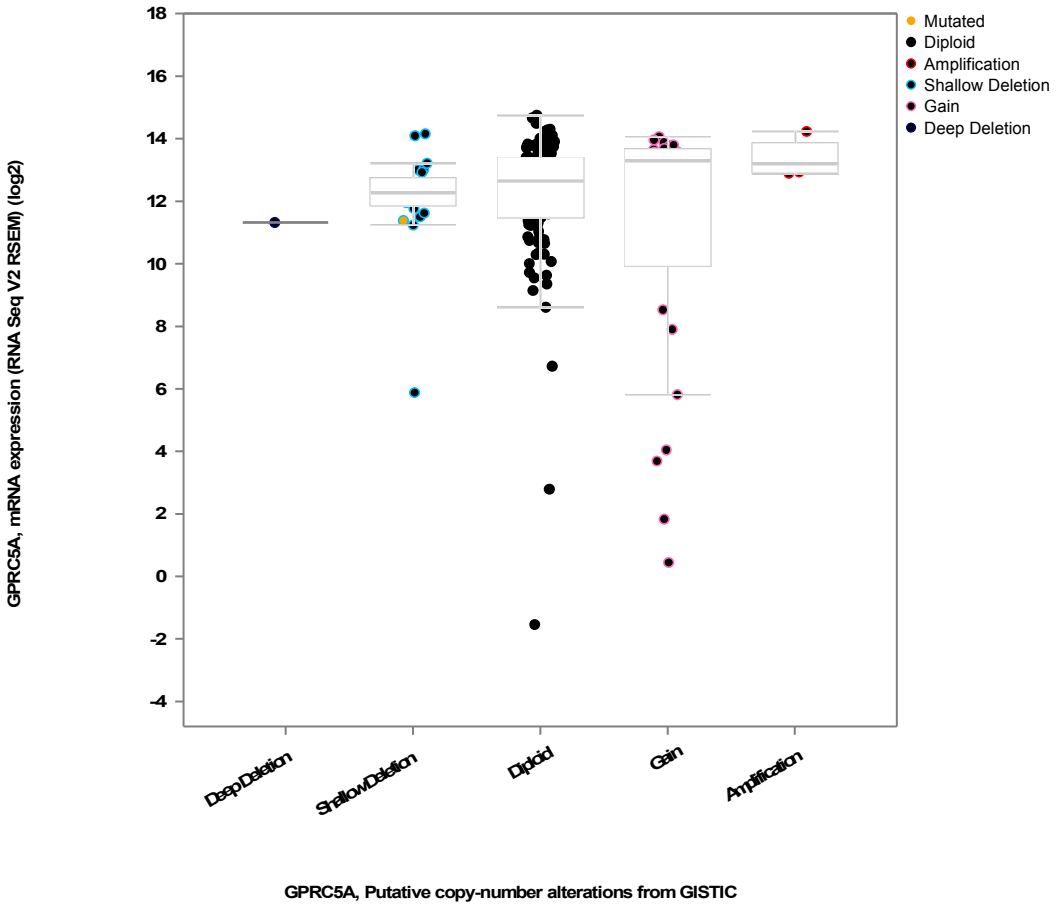

Figure 4.17 GPRC5A mRNA expression data compared to copy number alterations in PDAC

4.3 Discussion

Pancreatic Adenocarcinoma (PDAC) is the 4th leading cause of cancer-related death in the U.S., and it is projected that by 2020 it will be the 2nd most fatal cancer[49]. The low survival statistics for this disease suggest an urgent need for new therapies and early detection methods. Conventional therapies that target the tumor cells have proven largely unsuccessful due, at least in part, to the contribution of the tumor microenvironment to the aggressive pathology of PDAC[60]. We hypothesized that one or more GPCR drivers of this disease in the tumor cells or the CAFs could be identified by gene expression analysis.

G protein-coupled receptors (GPCRs) comprise up to 3% of the human genome and are both the largest protein receptor superfamily and the most common target of approved pharmacological agents[4,5,63]. A small number of GPCRs are currently targeted in cancer therapies. However, these receptors have been shown to play a role in autocrine/ paracrine signaling that drives cellular growth and tissue homeostasis, and are therefore targets to consider in the context of PDAC [4]. A broad-spectrum GPCR antagonist was shown to reduce growth and angiogenesis in PDAC, suggesting a role for GPCRs in the disease[14]. Utilizing an unbiased approach, TaqMan® GPCR array technology, I performed the first investigation of the GPCR expression profiles in PDAC and along with my colleague, Shu Zhou, of the CAFs from the surrounding microenvironment.

Array technology has been widely used to study gene expression in multiple tumor types, including PDAC, and has identified the differential expression of over 500 genes in the disease compared to normal tissue.[64] However, there has been poor agreement among the results due to variable tissue selection and processing, differing microarray methodologies, and a lack of standardized analysis and data mining. Furthermore, our laboratory has found that Affymetrix arrays are not an ideal method to assess GPCR expression levels[3]. For this reason, a GPCR-specific RT-PCR array (Life Technologies/ Applied Biosystems) was used in the studies described in this thesis

I found that tumor sections from multiple patients expressed a large number of GPCRs, sharing 73 of those detected in each (average of 45% similarity). Since whole tumor sections may include disproportional amounts of variable cell types, including stromal cells, vascular components, immune cells and cancer cells, we analyzed individual cell lines including two patient-derived cells lines (34E and 79E) and two widely used established cell lines (Aspc-1 and MiaPaCa-2). We found that the two patient-derived cell lines shared in the expression of 119 GPCRs, comprising 88% and 62% of the total GPCRs detected in each patient's cells. The two established cell lines shared 68 GPCRs, or 57% and 70% of each cell line's total detected GPCRs. Of these 68 GPCRs, 55 (81%) were also expressed in both of the patient cell lines. We also analyzed the GPCR expression profile on a normal epithelial ductal cell line (HPDE6) for the purpose of comparison to the disease cell lines.

There were only two GPCRs that were shared by all four PDAC cell lines but not detected on the normal cell line (classified as “unique” to the PDAC cell lines; Table 4.3). However, both of these GPCRs were expressed at relatively low levels in PDAC cells (ΔCt values near 25, the limit of detection) and therefore may not be functionally important or therapeutically advantageous targets. By identifying GPCRs with the largest increases in expression in the PDAC cells compared to the normal HPDE6 cells, we found two GPCRs that were shared among the PDAC samples and had >4-fold greater expression in PDAC compared to HPDE6. Brain angiogenesis inhibitor 1, BAI1, exhibited on average 22-fold higher expression, and GPRC5A, or retinoic acid-induced III (RAI3), had 33-fold higher expression in PDAC compared to HPDE6 cells. GPRC5A was also the mostly highly expressed GPCR shared among the three tumor samples and the four PDAC cell lines. We sought to identify a GPCR that might be highly expressed on both PDAC cells as well as the cancer-associated fibroblasts (CAFs). Indeed, GPRC5A was one of the mostly highly expressed GPCRs on five patient-derived CAF samples, and had 32-fold higher expression in these cells relative to pancreatic stellate cells (PSCs).

High throughput analysis is often suitable for large-scale data generation but also can generate false-positives, especially when one finds differential gene expression. Thus, it is critical to validate findings using independent methods. To confirm the GPCR array data, I designed primers and performed real-time PCR to confirm the high expression of GPRC5A in each sample that

been assayed using the GPCR array. The independent qPCR data for GPRC5A expression correlated well to that of the GPCR array (Figure 4.10). It would also be important to investigate if the changes in expression of mRNA for this target produce a differential expression pattern of protein expression on the PDAC cells compared to normal cells. However, limitations in the availability of established antibodies compared to the number of proteins in the human proteome make such analysis quite difficult[64]. Unfortunately, several antibodies used in this study have thus far failed internal control measures for immunodetection of GPRC5A.

After validating the increased expression of GPRC5A in PDAC compared to HPDE6 cells, I initiated studies to assess whether it functions to promote cancer cell proliferation, measured as DNA synthesis using [^{3}H]-thymidine incorporation of HPDE6 cells transiently transfected with GPRC5A or a vector control. I found that GPRC5A-overexpressing cells exhibited significantly increased DNA synthesis relative to vector control-transfected cells. This suggests a proliferative role of GPRC5A in pancreatic cells. Although we expected that overexpression of GPRC5A might also improve the viability of HPDE6 cells that overexpress it, this result was not observed. This may be a due to the act of transfection itself, which results in a drop of viability of about 30% for both transfected groups compared to untreated HPDE6 cells, with no significant difference between the two transfected groups. Perhaps a greater disparity in viability would be observed if it was measured at a later time point.

We utilized publicly available data such as the Cancer Genome Atlas (CGA) and the Gene Expression omnibus (GEO) to further investigate the expression profile of GPRC5A in various tissues, including pancreatic cancer. The GEO data indicate that GPRC5A is much more highly expressed in PDAC than in normal pancreatic tissue. However, copy number alterations or mutations are found in only 3.3% of 90 patients in TCGA as reported by the cBioPortal database. The largest changes in GPRC5A copy number are found in ovarian cancer, though there were alterations in many cancer types.

GPRC5A (alternatively known as RAI3 or RAIG1), was first described as a retinoic-acid inducible protein in the oral squamous carcinoma cell line UMSCC-22B and was shown to have substantial expression in the lung tissue of normal adults[65]. GPRC5A has proximal p53 and CREB binding domains as well as retinoic acid regulatory elements (RAREs) upstream of the transcriptional start site and has been shown to play a role in regulating the cell cycle[66]. Expression of GPRC5a is reportedly increased in KRAS mutant cells and up-regulated in cancers with mutated p53[67,68]. GPRC5A has a reciprocal relationship with intracellular cAMP: increased cellular cAMP elevates GPRC5A expression, resulting in a reduction in intracellular cAMP[69]. GPRC5A has been implicated in the pathogenesis and pathophysiology of multiple cancers. GPRC5A is up-regulated in breast cancer, where knockdown may reduce cancer cell growth[70]. It is highly expressed in the tumor epithelium in the colon, and a proteomic screen suggested that it may be used as a biomarker for colorectal cancer [71,72].

Interestingly, GPRC5A has been shown to act as a tumor suppressor in the lung, which suggests that it may have a tissue-specific role in cell-cycle control[73]. One report suggested that GPRC5A is phosphorylated via EGFR and inactivated in lung cancer but conversely another study found that GPRC5A negatively regulates EGFR [74,75], suggesting the two receptors may be partnered. These findings indicate that GPRC5A is potentially a central node in which cAMP, p53, KRAS, and EGFR- mediated malignant pathways converge; thus, it would be of interest to produce compounds that modulate GPRC5A activity.

As there is currently no known ligand or agonist for GPRC5A, and no crystal structure available for this molecule, I generated a predicted structural model of GPRC5A. Using I-TASSER, I found that GPRC5A shows closest analogy to other members of the class C metabotropic receptors, specifically metabotropic receptor 1 and 5 (mGluR1 and mGluR5). We anticipated close association with class C GPCRs, as GPRC5A had been classified as a member of this receptor subfamily. Both mGluR1 and mGluR5 signal via $G_{q/11}$[76], but linkage prediction based on the C-terminal sequence of GPRC5A (PredCouple-2) suggested that GPRC5A is likely to act via G_i. Class C GPCRs have distinct characteristics, including a N-terminus appendage or “Venus flytrap” which contain orthosteric binding sites that can be targeted therapeutically[76]. GPRC5A does not appear to have a large VFT. However, both mGluR1 and mGluR5 can be targeted with negative allosteric modulators that bind at allosteric sites that partially overlap with the orthosteric binding site (mGluR1) or within the

transmembrane domain (mGluR5)[77,78]. This suggests that there may be options to allosterically target GPRC5A. Relatively little work has been done to produce drugs that target this class of GPCRs, highlighting a direction for future studies. One potential option would be the use of antibodies, or their smaller cousins, nanobodies, which are advantageous due to their high affinity and specificity for their targets and have previously been used to target other GPCRs implicated in cancer (such as CXCR4)[79].

In conclusion, the current study is the first to define the GPCR expression profile of PDAC and resulted in the discovery of a target of interest, GPRC5A. We found substantial overlap in the GPCR expression profiles of individual patient tumors, two patient cell lines and two established PDAC cell lines. GPRC5A was identified as exhibiting the greatest up-regulation of the GPCRs that were shared and had increased expression in PDAC relative to the normal cell line HPDE6. Moreover, GPRC5A was the highest expressed GPCR on all cell lines that have been tested. GPRC5A is also up-regulated in pancreatic CAFs compared to PSCs and therefore may be a target with actions on the cancer cells themselves and on cells in its collaborative microenvironment. Increasing GPRC5A expression in a normal pancreatic ductal cell line increased DNA synthesis, indicating the receptor's potential as a driver of PDAC cell growth. Data from publicly available sources suggest that GPRC5A is more highly expressed in PDAC tumors than in normal tissue and that it has relatively low numbers of mutations or copy number alterations in PDAC. Based on prior

studies, GPRC5A may regulate multiple pathways that drive the malignant phenotype. As an orphan receptor, GPRC5A belongs to a class of GPCRs that were previously unrecognized as playing potentially important roles in physiology and disease but have not as-yet been targeted by pharmacological agents. The findings in this thesis suggest that it would be of value to develop therapeutic strategies that target GPRC5A, and that it may also have potential as a possible biomarker for PDAC.

References

1. Stockert, J. A. & Devi, L. A. Advancements in therapeutically targeting orphan GPCRs. *Front. Pharmacol.* **6,** 100 (2015).

2. Heng, B. C., Aubel, D. & Fussenegger, M. An overview of the diverse roles of G-protein coupled receptors (GPCRs) in the pathophysiology of various human diseases. *Biotechnol. Adv.* **31,** 1676–94 (2013).

3. Insel, P. A.,. GPCR Expression in Native Cells: 'Novel' endoGPCRs as Physiologic Regulators and Therapeutic Targets. *Mol. Pharmacol.* **88,** 181–187 (2015).

4. Heng, B. C., Aubel, D. & Fussenegger, M. An overview of the diverse roles of G-protein coupled receptors (GPCRs) in the pathophysiology of various human diseases. *Biotechnol. Adv.* **31,** 1676–1694 (2013).

5. Insel, P. A., Wilderman, A., Zambon, A., Snead, A. Murray, F. Aroonsakool, N., McDonald, D., Zhou, S., McCann, T., Zhang, L., Sriram, K., Chinn, A., Michkov, A.V., Lynch, R., Overland, A., Corriden, R. GPCR expression in tissues and cells: are the optimal receptors being used as drug targets? *Br. J. Pharmacol.* **165,** 1613–6 (2012).

6. Smrcka, A. V. G protein βγ subunits: central mediators of G protein-coupled receptor signaling. *Cell. Mol. Life Sci.* **65,** 2191–214 (2008).

7. O'Hayre, M., Degese, M. S. & Gutkind, J. S. Novel insights into G protein and G protein-coupled receptor signaling in cancer. *Curr. Opin. Cell Biol.* **27,** 126–35 (2014).

8. Dorsam, R. T. & Gutkind, J. S. G-protein-coupled receptors and cancer. *Nat. Rev. Cancer* **7,** 79–94 (2007).

9. O'Connor, K. & Chen, M. Dynamic functions of RhoA in tumor cell migration and invasion. *Small GTPases* **4,** 141–7

10. Zhou, X. & Zheng, Y. Cell type-specific signaling function of RhoA GTPase: lessons from mouse gene targeting. *J. Biol. Chem.* **288,** 36179–88 (2013).
11. Overland, A. C. & Insel, P. A. Heterotrimeric G Proteins Directly Regulate MMP14/Membrane Type-1 Matrix Metalloprotease: A Novel Mechanism for GPCR-EGFR Transactivation. *J. Biol. Chem.* **290,** 9941–7 (2015).

12. Pierce, K. L., Luttrell, L. M. & Lefkowitz, R. J. New mechanisms in heptahelical receptor signaling to mitogen activated protein kinase cascades. *Oncogene* **20,** 1532–9 (2001).

13. O'Hayre, M. Salanga, Catherina L., Kipps, Thomas J., Messmer, Davorka, Dorrestein, Pieter C., Handel, Tracy M. Elucidating the CXCL12/CXCR4 signaling network in chronic lymphocytic leukemia through phosphoproteomics analysis. *PLoS One* **5,** (2010).

14. Guha, S. Eibl, G., Kisfalvi, K., Fan, R.S., Burdick, M., Reber, H., Hines, O.J., Strieter, R., Rozengurt, E. Broad-spectrum G protein-coupled receptor antagonist, [D-Arg1,D-Trp5,7,9,Leu11]SP: a dual inhibitor of growth and angiogenesis in pancreatic cancer. *Cancer Res.* **65,** 2738–2745 (2005).

15. Furukawa, T. Duguid, W P Rosenberg, L Viallet, J Galloway, D a Tsao, M S. Long-term culture and immortalization of epithelial cells from normal adult human pancreatic ducts transfected by the E6E7 gene of human papilloma virus 16. *Am. J. Pathol.* **148,** 1763–1770 (1996).

16. Chae, H. J. Kang, J S Byun, J O Han, K S Kim, D U Oh, S M Kim, H M Chae, S W Kim, H R. Molecular mechanism of staurosporine-induced apoptosis in osteoblasts. *Pharmacol. Res.* **42,** 373–381 (2000).

17. Zhang, L., Lingzhi Murray, Fiona Zahno, Anja Kanter, Joan R Chou, Daisy Suda, Ryan Fenlon, Michael Rassenti, Laura Cottam, Howard Kipps, Thomas J Insel, Paul ACyclic nucleotide phosphodiesterase profiling reveals increased expression of phosphodiesterase 7B in chronic lymphocytic leukemia. *Proc. Natl. Acad. Sci. U. S. A.* **105,** 19532–7 (2008).

18. Zahno, A. C. Zahno, Anja Christina Murray, Fiona Zhang, Lingzhi Rassenti, Laura Cottam, Howard Kipps, Thomas Insel, Paul. Phosphodiesterase 7 (PDE7) and PDE4/7 inhibitors kill chronic lymphocytic leukemia (CLL) cells via a cAMP-mitochondrial-dependent pathway. *FASEB J* **23,** 761.10–(2009).

19. Crook, R. B. & Stanley B., P. Vasoactive intestinal peptide stimulates cyclic AMP metabolism in choroid plexus epithelial cells. *Brain Res.* **384,** 138–144 (1986).

20. Tatro, J. B. Receptor biology of the melanocortins, a family of neuroimmunomodulatory peptides. *Neuroimmunomodulation* **3,** 259–84

21. Verduyn, C. Verduyn, C Van Kleef, R Frank, J Schreuder, H Van Dijken, J P Scheffers, W A. Properties of the NAD(P)H-dependent xylose reductase from the xylose-fermenting yeast Pichia stipitis. *Biochem. J.* **226,** 669–77 (1985).

22. Burns, J. A., Butler, J. C., Moran, J. & Whitesides, G. M. Selective reduction of disulfides by tris(2-carboxyethyl)phosphine. *J. Org. Chem.* **56,** 2648–2650 (1991).

23. Ghorbani, A. Ghorbani, Arman Jeddi-Tehrani, Mahmood Saidpour, Atoosa Safa, Majid Bayat, Ahmad Ali Zand, Hamid. PI3K/AKT and Mdm2 activation are associated with inhibitory effect of cAMP increasing agents on DNA damage-induced cell death in human pre-B NALM-6 cells. *Arch. Biochem. Biophys.* **566,** 58–66 (2015).

24. Gekel, I. & Neher, E. Application of an Epac activator enhances neurotransmitter release at excitatory central synapses. *J. Neurosci.* **28,** 7991–8002 (2008).

25. Lu, D., Aroonsakool, N., Yokoyama, U., Patel, H. H. & Insel, P. A. Increase in cellular cyclic AMP concentrations reverses the profibrogenic phenotype of cardiac myofibroblasts: a novel therapeutic approach for cardiac fibrosis. *Mol. Pharmacol.* **84,** 787–93 (2013).

26. Siegel, R. L., Miller, K. D. & Jemal, A. Cancer statistics, 2015. *CA. Cancer J. Clin.* **65,** 5–29 (2015).

27. Malek, S. Molecular biomarkers in chronic lymphocytic leukemia. *Adv. Exp. Med. Biol.* **792,** 193–214 (2013).

28. Bertilaccio, M. T. S., Scielzo, C., Muzio, M. & Caligaris-Cappio, F. An overview of chronic lymphocytic leukaemia biology. *Best Pract. Res. Clin. Haematol.* **23,** 21–32 (2010).

29. Keating, M. J. Biology and Treatment of Chronic Lymphocytic Leukemia. *Hematology* **2003,** 153–175 (2003).

30. Kitada, S., Andersen, J Akar, S Zapata, J M Takayama, S Krajewski, S Wang, H G Zhang, X Bullrich, F Croce, C M Rai, K Hines, J Reed, J C. Expression of apoptosis-regulating proteins in chronic lymphocytic leukemia: correlations with In vitro and In vivo chemoresponses. *Blood* **91,** 3379–89 (1998).

31. Hallek, M, Bruce D. Catovsky, Daniel Caligaris-Cappio, Federico Dighiero, Guillaume Döhner, Hartmut Hillmen, Peter Keating, Michael J. Montserrat, Emili Rai, Kanti R. Kipps, Thomas J.. Guidelines for the diagnosis and treatment of chronic lymphocytic leukemia: A report from the International Workshop on Chronic Lymphocytic Leukemia updating the National Cancer Institute-Working Group 1996 guidelines. *Blood* **111,** 5446–5456 (2008).

32. Nabhan, C. & Rosen, S. T. Chronic Lymphocytic Leukemia. *JAMA* **312,** 2265 (2014).

33. Yokoyama, U., Patel, Hemal H Lai, N Chin Aroonsakool, Nakon Roth, David M Insel, Paul A. The cyclic AMP effector Epac integrates pro- and anti-fibrotic signals. *Proc. Natl. Acad. Sci. U. S. A.* **105,** 6386–91 (2008).

34. Omori, K. & Kotera, J. Overview of PDEs and their regulation. *Circ. Res.* **100,** 309–27 (2007).

35. Monahan, T. M., Marchand, N. W., Fritz, R. R. & Abell, C. W. Cyclic adenosine 3':5'-monophosphate levels and activities of related enzymes in normal and leukemic lymphocytes. *Cancer Res.* **35,** 2540–7 (1975).

36. Murray, F. & Insel, P. A. Targeting cAMP in chronic lymphocytic leukemia: a pathway-dependent approach for the treatment of leukemia and lymphoma. *Expert Opin. Ther. Targets* **17,** 937–49 (2013).

37. Siegmund, B. Welsch, J Loher, F Meinhardt, G Emmerich, B Endres, S Eigler, A. Phosphodiesterase type 4 inhibitor suppresses expression of anti-apoptotic members of the Bcl-2 family in B-CLL cells and induces caspase-dependent apoptosis. *Leukemia* **15,** 1564–71 (2001).

38. Tiwari, S. Felekkis, Kyriacos Moon, Eun-Yi Flies, Amanda Sherr, David H Lerner, Adam. Among circulating hematopoietic cells, B-CLL uniquely expresses functional EPAC1, but EPAC1-mediated Rap1 activation does not account for PDE4 inhibitor-induced apoptosis. *Blood* **103,** 2661–7 (2004).

39. Anthony, B. A. & Link, D. C. Regulation of hematopoietic stem cells by bone marrow stromal cells. *Trends Immunol.* **35,** 32–7 (2014).

40. Ten Hacken, E. & Burger, J. A. Molecular pathways: targeting the microenvironment in chronic lymphocytic leukemia--focus on the B-cell receptor. *Clin. Cancer Res.* **20,** 548–56 (2014).

41. Balakrishnan, K. Burger, Jan A Quiroga, Maite P Henneberg, Marina Ayres, Mary L Wierda, William G Gandhi, Varsha. Influence of bone marrow stromal microenvironment on forodesine-induced responses in CLL primary cells. *Blood* **116,** 1083–91 (2010).

42. Manshouri, T. Estrov, Zeev Quintás-Cardama, Alfonso Burger, Jan Zhang, Ying Livun, Ana Knez, Liza Harris, David Creighton, Chad J. Kantarjian, Hagop M. Verstovsek, Srdan. Bone marrow stroma-secreted cytokines protect JAK2V617F-mutated cells from the effects of a JAK2 inhibitor. *Cancer Res.* **71,** 3831–3840 (2011).

43. Kurtova, A. V. Balakrishnan, Kumudha Chen, Rong Ding, Wei Schnabl, Susanne Quiroga, Maite P. Sivina, Mariela Wierda, William G. Estrov, Zeev Keating, Michael J. Shehata, Medhat Jäger, Ulrich Gandhi, Varsha Kay, Neil E. Plunkett, William Burger, Jan., Diverse marrow stromal cells protect CLL cells from spontaneous and drug-induced apoptosis: Development of a reliable and reproducible system to assess stromal cell adhesion-mediated drug resistance. *Blood* **114,** 4441–4450 (2009).

44. Zhang, W. Trachootham, Dunyaporn Liu, Jinyun Chen, Gang Pelicano, Helene Garcia-Prieto, Celia Lu, Weiqin Burger, Jan A Croce, Carlo M Plunkett, William Keating, Michael J Huang, Peng. Stromal control of cystine metabolism promotes cancer cell survival in chronic lymphocytic leukaemia. *Nat. Cell Biol.* **14,** 276–86 (2012).

45. Janel, A. Dubois-Galopin, Frédérique Bourgne, Céline Berger, Juliette Tarte, Karin Boiret-Dupré, Nathalie Boisgard, Stéphane Verrelle, Pierre Déchelotte, Pierre Tournilhac, Olivier Berger, Marc G. The chronic lymphocytic leukemia clone disrupts the bone marrow microenvironment. *Stem Cells Dev.* **23,** 2972–82 (2014).

46. Kawano, Y. Kobune, Masayoshi Yamaguchi, Miki Nakamura, Kiminori Ito, Yoshinori Sasaki, Katsunori Takahashi, Sho Nakamura, Takafumi Chiba, Hiroki Sato, Tsutomu Matsunaga, Takuya Azuma, Hiroshi Ikebuchi, Kenji Ikeda, Hisami Kato, Junji Niitsu, Yoshiro Hamada, Hirofumi. Ex vivo expansion of human umbilical cord hematopoietic progenitor cells using a coculture system with human telomerase catalytic subunit (hTERT)-transfected human stromal cells. *Blood* **101,** 532–540 (2003).

47. Jarvis, L. J., Maguire, J. E. & LeBien, T. W. Contact between human bone marrow stromal cells and B lymphocytes enhances very late antigen-4/vascular cell adhesion molecule-1-independent tyrosine phosphorylation of focal adhesion kinase, paxillin, and ERK2 in stromal cells. *Blood* **90,** 1626–35 (1997).

48. Jarvis, L. J. & LeBien, T. W. Stimulation of human bone marrow stromal cell tyrosine kinases and IL-6 production by contact with B lymphocytes. *J. Immunol.* **155,** 2359–68 (1995).

49. Rahib, L. Smith, Benjamin D Aizenberg, Rhonda Rosenzweig, Allison B Fleshman, Julie M Matrisian, Lynn M. Projecting cancer incidence and deaths to 2030: the unexpected burden of thyroid, liver, and pancreas cancers in the United States. *Cancer Res.* **74,** 2913–21 (2014).

50. Siegel, R., Naishadham, D. & Jemal, A. Cancer statistics, 2013. *CA. Cancer J. Clin.* **63,** 11–30 (2013).

51. Sclafani, F., Iyer, R., Cunningham, D. & Starling, N. Management of metastatic pancreatic cancer: Current treatment options and potential new therapeutic targets. *Crit. Rev. Oncol. Hematol.* (2015). doi:10.1016/j.critrevonc.2015.03.008

52. Halkova, T., Cuperkova, R., Minarik, M. & Benesova, L. MicroRNAs in Pancreatic Cancer: Involvement in Carcinogenesis and Potential Use for Diagnosis and Prognosis. *Gastroenterol. Res. Pract.* **2015,** 892903 (2015).

53. Paulson, A. S., Tran Cao, H. S., Tempero, M. A. & Lowy, A. M. Therapeutic advances in pancreatic cancer. *Gastroenterology* **144,** 1316–26 (2013).

54. Hruban, R. H. & Klimstra, D. S. Adenocarcinoma of the pancreas. *Semin. Diagn. Pathol.* **31,** 443–51 (2014).

55. Pancreatic Adenocarcinoma — NEJM. at <http://www.nejm.org/doi/full/10.1056/NEJMra1404198>

56. Neesse, A., Krug, S., Gress, T. M., Tuveson, D. A. & Michl, P. Emerging concepts in pancreatic cancer medicine: targeting the tumor stroma. *Onco. Targets. Ther.* **7,** 33–43 (2013).

57. Neesse, A., Krug, S., Gress, T. M., Tuveson, D. a. & Michl, P. Emerging concepts in pancreatic cancer medicine: Targeting the tumor stroma. *Onco. Targets. Ther.* **7,** 33–43 (2013).

58. Neesse, A., Algül, H., Tuveson, D. A. & Gress, T. M. Stromal biology and therapy in pancreatic cancer: a changing paradigm. *Gut* gutjnl–2015–309304– (2015). doi:10.1136/gutjnl-2015-309304

59. Phillips, P. Pancreatic stellate cells and fibrosis. (2012). at <http://www.ncbi.nlm.nih.gov/books/NBK98937/>

60. McCarroll, J. A. McCarroll, Joshua A Naim, Stephanie Sharbeen, George Russia, Nelson Lee, Julia Kavallaris, Maria Goldstein, David Phillips, Phoebe A. Role of pancreatic stellate cells in chemoresistance in pancreatic cancer. *Front. Physiol.* **5,** 141 (2014).

61. Kikuta, K. Masamune, Atsushi Watanabe, Takashi Ariga, Hiroyuki Itoh, Hiromichi Hamada, Shin Satoh, Kennichi Egawa, Shinichi Unno, Michiaki Shimosegawa, Tooru. Pancreatic stellate cells promote epithelial-mesenchymal transition in pancreatic cancer cells. *Biochem. Biophys. Res. Commun.* **403,** 380–384 (2010).

62. Jianyi Yang1, Renxiang Yan1, Ambrish Roy1, D. X. & Jonathan Poisson1 & Yang Zhang1, 2. The I-TASSER Suite: protein structure and function prediction. *Nature methods* at <http://zhanglab.ccmb.med.umich.edu/papers/2015_1.pdf>

63. Insel, P. A., Tang, C.-M., Hahntow, I. & Michel, M. C. Impact of GPCRs in clinical medicine: monogenic diseases, genetic variants and drug targets. *Biochim. Biophys. Acta* **1768,** 994–1005 (2007).

64. Grützmann, R. Saeger, Hans Detlev Lüttges, Jutta Schackert, Hans Konrad Kalthoff, Holger Klöppel, Günter Pilarsky, Christian. Microarray-based gene expression profiling in pancreatic ductal carcinoma: status quo and perspectives. *Int. J. Colorectal Dis.* **19,** 401–413 (2004).

65. Cheng, Y. Molecular Cloning and Characterization of a Novel Retinoic Acid-inducible Gene That Encodes a Putative G Protein-coupled Receptor. *J. Biol. Chem.* **273,** 35008–35015 (1998).

66. Zhou, H. & Rigoutsos, I. The emerging roles of GPRC5A in diseases. *Oncoscience* **1,** 765–76 (2014).

67. Qian, J., Niu, J., Li, M., Chiao, P. J. & Tsao, M.-S. In vitro modeling of human pancreatic duct epithelial cell transformation defines gene expression changes induced by K-ras oncogenic activation in pancreatic carcinogenesis. *Cancer Res.* **65,** 5045–53 (2005).

68. Wu, Q. Ding, Wei Mirza, Asra Van Arsdale, Tish Wei, Iris Bishop, W. Robert Basso, Andrea McClanahan, Terri Luo, Lin Kirschmeier, Paul Gustafson, Eric Hernandezi, Marco Liu, Suxing. Integrative genomics revealed RAI3 is a cell growth-promoting gene and a novel P53 transcriptional target. *J. Biol. Chem.* **280,** 12935–12943 (2005).

69. Hirano, M. Zang, Liqing Oka, Takehiko Ito, Yoshiyuki Shimada, Yasuhito Nishimura, Yuhei Tanaka, Toshio. Novel reciprocal regulation of cAMP signaling and apoptosis by orphan G-protein-coupled receptor GPRC5A gene expression. *Biochem. Biophys. Res. Commun.* **351,** 185–191 (2006).

70. Nagahata, T. Sato, T. Tomura, A. Onda, M. Nishikawa, K. Emi, M.. Identification of RAI3 as a therapeutic target for breast cancer. *Endocr. Relat. Cancer* **12,** 65–73 (2005).

71. Zougman, A. Hutchins, Gordon G Cairns, David A Verghese, Eldo Perry, Sarah L Jayne, David G Selby, Peter J Banks, Rosamonde E. Retinoic acid-induced protein 3: identification and characterisation of a novel prognostic colon cancer biomarker. *Eur. J. Cancer* **49,** 531–9 (2013).

72. Kume, H. Muraoka, Satoshi Kuga, Takahisa Adachi, Jun Narumi, Ryohei Watanabe, Shio Kuwano, Masayoshi Kodera, Yoshio Matsushita, Kazuyuki Fukuoka, Junya Masuda, Takeshi Ishihama, Yasushi Matsubara, Hisahiro Nomura, Fumio Tomonaga, Takeshi. Discovery of colorectal cancer biomarker candidates by membrane proteomic analysis and subsequent verification using selected reaction monitoring (SRM) and tissue microarray (TMA) analysis. *Mol. Cell. Proteomics* **13,** 1471–84 (2014).

73. Acquafreda, T., Soprano, K. J. & Soprano, D. R. GPRC5A: A potential tumor suppressor and oncogene. *Cancer Biol. Ther.* **8,** 963–965 (2009).

74. Zhong, S. Yin, Huijing Liao, Yueling Yao, Feng Li, Qi Zhang, Jie Jiao, Huike Zhao, Yongxu Xu, Dongliang Liu, Shuli Song, Hongyong Gao, Yong Liu, Jingyi Ma, Lina Pang, Zhi Yang, Ruixu Ding, Chengyi Sun, Beibei Lin, Xiaofeng Ye, Xiaofeng Guo, Wenzheng Han, Baohui Zhou, Binhua P Chin, Y Eugene Deng, Jiong. Lung Tumor Suppressor GPRC5A Binds EGFR and Restrains Its Effector Signaling. *Cancer Res.* **75,** 1801–14 (2015).

75. Lin, X. Zhong, Shuangshuang Ye, Xiaofeng Liao, Yueling Yao, Feng Yang, Xiaohua Sun, Beibei Zhang, Jie Li, Qi Gao, Yong Wang, Yifan Liu, Jingyi Han, Baohui Chin, Y Eugene. EGFR phosphorylates and inhibits lung tumor suppressor GPRC5A in lung cancer. 1–12 (2014).

76. Chun, L., Zhang, W. & Liu, J. Structure and ligand recognition of class C GPCRs. *Acta Pharmacol. Sin.* **33,** 312–23 (2012).

77. Structure of a Class C GPCR Metabotropic Glutamate Receptor 1 Bound to an Allosteric Modulator . at <http://www.meilerlab.org/index.php/publications/showPublication/pub_id/166>

78. Conn, P. J., Christopoulos, A. & Lindsley, C. W. Allosteric modulators of GPCRs: a novel approach for the treatment of CNS disorders. *Nat. Rev. Drug Discov.* **8,** 41–54 (2009).

79. Mujić-Delić, A., de Wit, R. H., Verkaar, F. & Smit, M. J. GPCR-targeting nanobodies: attractive research tools, diagnostics, and therapeutics. *Trends Pharmacol. Sci.* **35,** 247–55 (2014).